AD_____

Award Number: W81XWH-10-1-0051

TITLE: Hsf1 in Her2-Positive Breast Cancer

PRINCIPAL INVESTIGATOR: Michael Sherman, Ph.D.

CONTRACTING ORGANIZATION: Boston University, Boston, MA 02118-2436

REPORT DATE: October 2012

TYPE OF REPORT: Final

PREPARED FOR: U.S. Army Medical Research and Materiel Command
                            Fort Detrick, Maryland 21702-5012

DISTRIBUTION STATEMENT: Approved for Public Release;
                                           Distribution Unlimited

The views, opinions and/or findings contained in this report are those of the author(s) and should not be construed as an official Department of the Army position, policy or decision unless so designated by other documentation.

REPORT DOCUMENTATION PAGE

Form Approved
OMB No. 0704-0188

Public reporting burden for this collection of information is estimated to average 1 hour per response, including the time for reviewing instructions, searching existing data sources, gathering and maintaining the data needed, and completing and reviewing this collection of information. Send comments regarding this burden estimate or any other aspect of this collection of information, including suggestions for reducing this burden to Department of Defense, Washington Headquarters Services, Directorate for Information Operations and Reports (0704-0188), 1215 Jefferson Davis Highway, Suite 1204, Arlington, VA 22202-4302. Respondents should be aware that notwithstanding any other provision of law, no person shall be subject to any penalty for failing to comply with a collection of information if it does not display a currently valid OMB control number. **PLEASE DO NOT RETURN YOUR FORM TO THE ABOVE ADDRESS.**

1. REPORT DATE October 2012	2. REPORT TYPE Final	3. DATES COVERED 15January2010–14September2012

4. TITLE AND SUBTITLE	5a. CONTRACT NUMBER
Hsf1 in Her2-Positive Breast Cancer	5b. GRANT NUMBER Y Ì 1ÝY PË €Ë Ë̈€í 1
	5c. PROGRAM ELEMENT NUMBER

6. AUTHOR(S)	5d. PROJECT NUMBER
Michael Sherman, Ph.D.	5e. TASK NUMBER
	5f. WORK UNIT NUMBER
E-Mail: sherma1@bu.edu	

7. PERFORMING ORGANIZATION NAME(S) AND ADDRESS(ES)	8. PERFORMING ORGANIZATION REPORT NUMBER
Boston University Boston, MA 02118-2436	

9. SPONSORING / MONITORING AGENCY NAME(S) AND ADDRESS(ES)	10. SPONSOR/MONITOR'S ACRONYM(S)
U.S. Army Medical Research and Materiel Command Fort Detrick, Maryland 21702-5012	
	11. SPONSOR/MONITOR'S REPORT NUMBER(S)

12. DISTRIBUTION / AVAILABILITY STATEMENT
Approved for Public Release; Distribution Unlimited

13. SUPPLEMENTARY NOTES

14. ABSTRACT

This study demonstrates that Hsf1 controls development of Her2-positive cancer both at the stage of initiation, via control of the oncogene-induced senescence, and progression, via regulation of tumor angiogenesis. It also dissects the mechanism of effects of Hsf1 on tumor angiogenesis, and demonstrates that Hsf1 regulates expression of the major angiogenesis factor HIF-1, and this regulation involves the translation regulator HuR. This program provides rationale for development of Hsf1 inhibitors that can inhibit multiple pathways in tumor initiation and progression. It also establishes a simple xenograft model that can be used for anti-Hsf1 drug testing.

15. SUBJECT TERMS
Hsf1, Her2 positive cancer, angiogenesis, Hif1

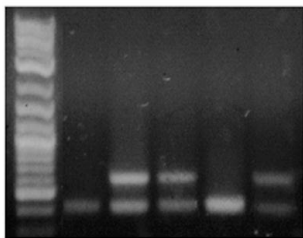| 16. SECURITY CLASSIFICATION OF:			17. LIMITATION OF ABSTRACT	18. NUMBER OF PAGES	19a. NAME OF RESPONSIBLE PERSON USAMRMC
a. REPORT U	b. ABSTRACT U	c. THIS PAGE U	UU	38	19b. TELEPHONE NUMBER *(include area code)*

Table of Contents

Introduction

It was previously demonstrated that tumorigenesis in several models strictly requires the heat shock transcription factor Hsf1. Indeed crossing of $p53^{-/-}$ mice with $hsf^{-/-}$ mice almost completely prevented lymphoma development (Min et al, 2007), but not appearance of some other cancers. Similarly, Hsf1 deficiency drastically delayed chemical skin carcinogenesis and increased survival from 30% to 90% (Dai et al, 2007). In this study, using transgenic and xenograft models, we uncovered that Hsf1 plays a critical role in development of Her2-positive breast cancer. Preliminary data suggested that Hsf1 is necessary for suppression of the oncogene-induced senescence (OIS), and for tumor angiogenesis. The major goal of this program was to investigate the molecular nature of these effects. Our data were corroborated by recently published population studies that Hsf1 is strongly upregulated in Her2-positive breast cancer and its levels correlate with poor prognosis (Santagata et al, 2012).

Body

Task 1

Hsf1 knockout suppresses Her2-induced hyperplasia and tumor development

We have previously found that the knockdown of Hsf1 in MCF10A human mammary epithelial cells prevents neoplastic transformation by Her2 oncogene. Indeed, while expression of Her2 in control MCF10A cells facilitated foci formation in culture and tumor appearance in nude mice, expression of this oncogene in Hsf1 knockdown MCF10A cells led to growth arrest and OIS, and tumors could not form in nude mice (Meng et al, 2010). To further dissect where in the tumorigenic process Hsf1 exerts its activity, here we used the transgenic animal model. We crossed Hsf1 knockout animals with mice expressing Her2/NeuT (a rodent homolog of Her2 carrying activating mutation) under the control of MMTV promoter (MMTVneu) (Guy et al, 1992) to generate WT-MMTVneu$^+$, hsf1$^{+/-}$MMTVneu$^+$, and hsf1$^{-/-}$MMTVneu$^+$ mice.

Hsf1 -/- +/- +/- -/- +/-
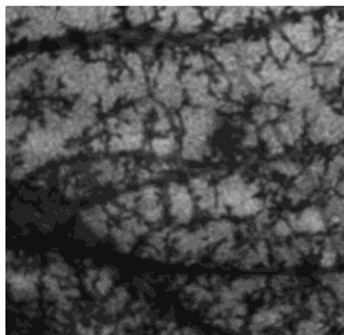
Fig. 1. Lack of Hsf1 in the knockout animals is shown by PCR.

MMTVneu
WT

MMTVneu
Hsf1 KO
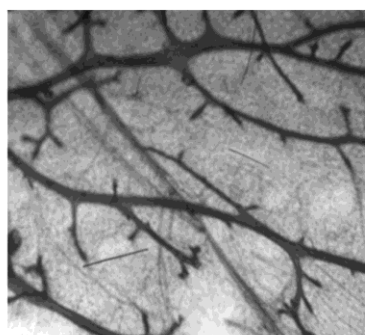
Fig. 2 Knockout of Hsf1 blocks NeuT-induced mammary duct and alveoli branching. WT-MMTVneu$^+$ and hsf1$^{-/-}$ MMTVneu$^+$ mice were sacrificed at 3-months of age and their mammary gland whole mounts were observed after Carnoy's fixative and staining with carmine.

To investigate the role of Hsf1 in Her2-induced hyperplasia, mammary glands were taken from 3-month old virgin mice to evaluate duct branching. Expression of Her2 in WT-MMTVneu$^+$ mammary gland led to high density of ducts and extensive alveoli branching, as reported previously (Muller et al, 1996). Importantly, hsf1$^{-/-}$MMTVneu$^+$ animals there was a low duct density, and almost no alveoli branching (Fig. 2). Therefore, Hsf1 KO prevented Her2-induced tissue hyperplasia, possibly by aggravating senescence, similar to what we have found recently with NeuT-induced mammary tumors in the Hsp72 knockout mouse model (Meng et al, 2011).
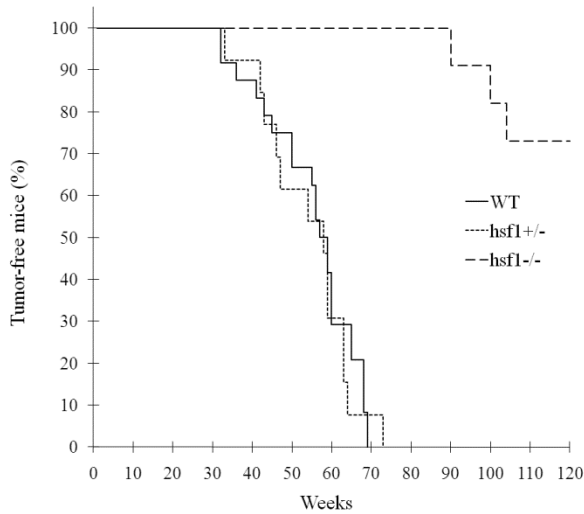
Fig. 3 Emergence of NeuT-induced tumors in WT-MMTVneu$^+$ (n=16), heterozygotes hsf1$^{+/-}$MMTVneu$^+$ (n=13), and hsf1$^{-/-}$MMTVneu$^+$ (n=11) animals.

To address whether Hsf1 KO suppresses NeuT-dependent tumorigenesis *in vivo,* we analyzed effects of hsf1 knockout on NeuT-induced tumor development. There was similar tumor incidence between heterozygous hsf1$^{+/-}$MMTVneu$^+$ and WT-MMTVneu$^+$ mice (median tumor appearance in this strain was about 55 weeks), indicating that one copy of the Hsf1 gene is sufficient to support mammary tumor emergence induced by Her2/NeuT (Fig. 3). In contrast, the absence of Hsf1 in homozygous knockout animals markedly inhibited mammary tumor development (Fig. 3). Indeed, tumors emerged with strong delay, and only three tumors of eleven animals appeared. Therefore, this model of Her2-positive breast cancer establishes that Hsf1 is critical for tumor initiation and hyperplasia.

To understand how Hsf1 suppresses tumor emergence, we investigated effects of Hsf1 knockdown on the Her2-induced senescence in the human mammary epithelial cells MCF10A. Knockdown of

Hsf1 did not significantly affect growth or senescence of these cells. Her2 transformed these cells. However, expression of Her2 in cells with knockdown of hsf1 led to growth arrest and senescence, indicating that Hsf1 depletion can precipitate the oncogene-induced senescence (Fig. 4).
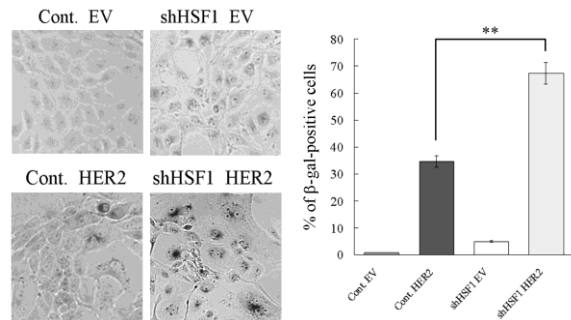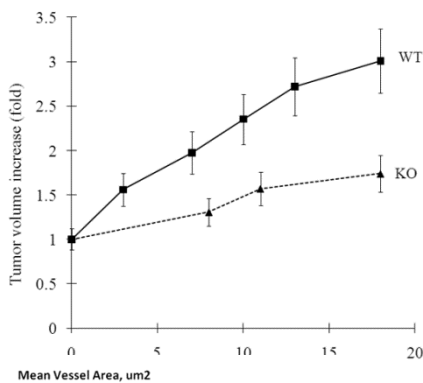
Fig. 4. HER2 triggers senescence in HSF1-deficient MCF-10A cells. β-galactosidase activity staining of MCF-10A control population (Cont.) and shHSF1 MCF-10A cells with (HER2) or without (empty vector, EV) HER2 overexpression. Right panel shows quantification of data shown in the left panel.

Task 2

Hsf1 knockdown suppresses tumor growth and angiogenesis

To investigate whether Hsf1 has additional effects on later stages of tumor development, we measured growth rates of rare tumors that emerge in hsf1 KO animals compared to control mice. Indeed, these tumors grew significantly slower than in control animals (Fig. 5) indicating that Hsf1 may be required not only for NeuT-induced initial transformation, but for tumor progression as well.

Fig. 5 NeuT-induced tumors in Hsf1 KO mice demonstrate reduce growth rate. The data shown are means +/-SEM.

Since among major factors limiting growth of solid tumors *in vivo* is neovascularization, we excised tumors from control and knockout animals, prepared slides and immunostained them with a marker of

5
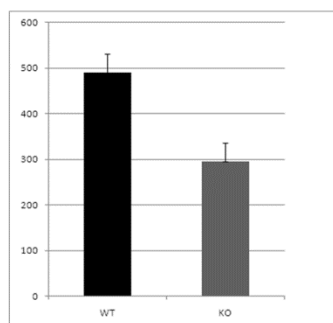
angiogenesis (endothelial cells) CD31. We observed that although the number of blood vessels was similar in wt and k/o animals (not shown), the mean vessel area in tumors from Hsf1 knockout animals was almost twice as low as in wild type animals (Fig. 6,7), indicating that the vessels were underdeveloped.

Fig. 6 Tumors in Hsf1 KO mice demonstrate reduced angiogenesis. Tumors from WT and KO animals were excised, fixed, stained for endothelial marker CD31, and analyzed for mean vessel area.

Fig. 7 Tumor tissue staining with anti-CD31 antibody. Tumors from control and Hsf1 KO animals are shown.

WT   hsf1 KO

Task 3

Hsf1 knockdown suppresses tumor growth and angiogenesis in xenograft model

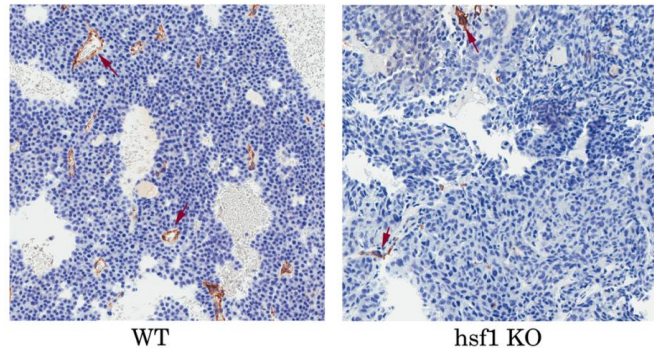Since in transgenic mouse model Hsf1 is lacking both in mammary tumor and surrounding stroma, to understand mechanisms by which Hsf1 can regulate angiogenesis we decided to switch from NeuT-induced mouse mammary tumors to a simpler system, i.e. xenograft with human breast cancer cells following Hsf1 knockdown. In this system Hsf1 can be downregulated specifically in human tumor cells but remain expressed normally in surrounding mouse stroma. As we reported previously, growth of many cancer cell lines (e.g. NeuT-expressing MCF10A cells or MDA-MB453) is dependent on Hsf1, since Hsf1 knockdown causes senescence due to accumulation of p21 and downregulation of the mitotic and anti-apoptotic protein survivin (Meng et al, 2010). Therefore these cell lines cannot propagate even in vitro upon depletion of Hsf1, and, accordingly, effects of Hsf1 on angiogenesis cannot be studied in this system.
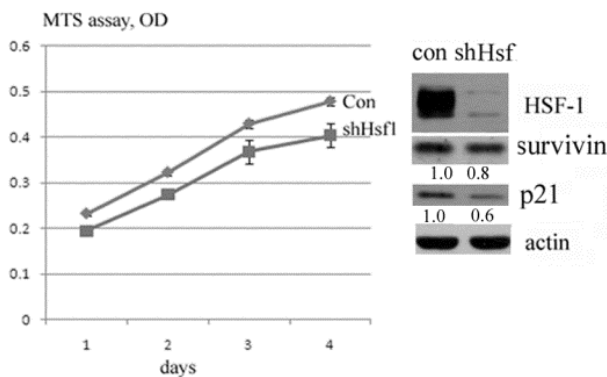
Fig. 8 Knockdown of Hsf1 has a little effect on growth of MCF7 cells in vitro and it does not increase p21 or decrease survivin levels. Cells were infected with shHsf1 retrovirus and selected for 4 days; their growth was assessed by MTS assay, and expression of p21 and survivin by immunoblotting.

To avoid this problem, we screened several breast tumor cell lines and found that Hsf1 knockdown does not decrease survivin levels and does not increase p21 levels in MCF7 human breast carcinoma (Fig. 8). Accordingly, growth of these cells in vitro was not significantly affected by Hsf1 knockdown (Fig. 8).

Therefore, we have chosen MCF7 cells to assess effect of Hsf1 knockdown on tumor angiogenesis and growth *in vivo* in the xenograft model. MCF7 cells were infected with retroviral vector expressing shHsf1 as described before and selected with puromycin for 5 days. To avoid possible variations of host factor(s) which could affect tumor growth, control cells were injected in right flanks and shHsf1 knockdown cells – in left flanks of the same animals and their growth was monitored by caliper. Tumors emerged at the sites of injection of both control and Hsf1-depleted cells on day 9 after inoculation (Fig. 9). Importantly, after tumor emergence, tumors formed by control MCF7 cells grew rapidly, while tumors formed by the Hsf1 knockdown ceased to grow soon after emergence (Fig. 9). The strong inhibitory effect of Hsf1 knockdown on growth of MCF7 cells in xenografts was in sharp contrast with cell culture, where Hsf1 knockdown practically did not affect the growth rate (Fig. 8). We have isolated tumors, stained them for CD31 as described above, and found that, similar to NeuT-induced mammary tumors in Hsf1 KO mice, Hsf1 knockdown markedly decreased mean vessel area in MCF7 human breast cancer xenografts (Fig. 10) (of note, there was no significant difference in the number of vessels). These data indicate that the xenograph model recapitulates effects of Hsf1 seen in transgenic model, and suggest that control of tumor angiogenesis may represent an important factor regulated by Hsf1.
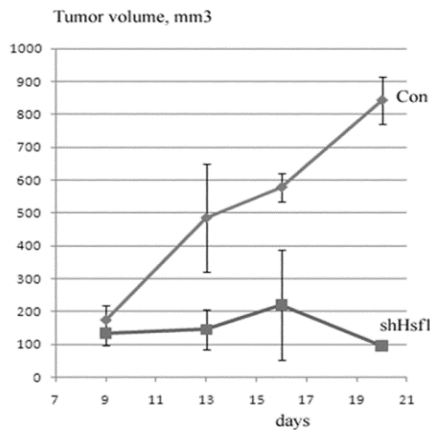
Fig. 9 Knockdown of Hsf1 blocks growth of MCF7 cells *in vivo* in xenografts. Cells infected with shHsf1 retrovirus as in A were injected in nude mice (10^6 cells per injection) and growth of tumors was monitored by caliper.
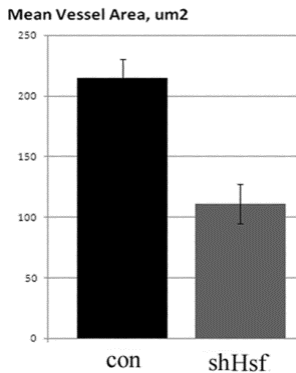
Fig. 10 Xenograft tumors from animals (as described in Fig. 8) were excised, fixed, stained for CD31 and analyzed for mean vessel area as in Fig. 6. Data are means+/-SE.

Hsf1 controls expression of the hypoxia-inducible factor HIF-1

Hypoxia-inducible factor 1 HIF-1 is considered to be the major regulator of tumor angiogenesis (Gordan & Simon, 2007; Semenza, 2009), and therefore we assessed its expression in xenografts formed by MCF7 cells with Hsf1 knockdown. We found high levels of HIF-1 in control tumors (which indicated hypoxic conditions in xenografts) but in tumors with Hsf1 knockdown there were much lower levels of HIF-1□ (Fig. 11). Similarly, in Hsf1 knockdown tumors we observed downregulation of HIF-1 target CAIX (carbonic anhydrase 9) (Fig. 11). Accordingly, Hsf1 appears to control angiogenesis in xenografts via regulating accumulation of HIF-1□.
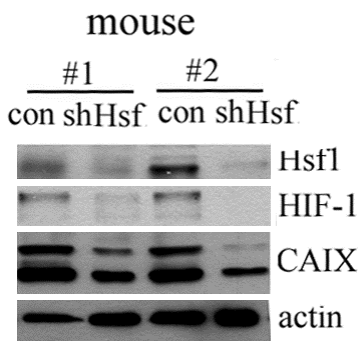
Fig. 11 Knockdown of Hsf1 reduces expression of HIF-1 and its target CAIX in xenografts. Expression of HIF-1 and CAIX tumor xenografts was analyzed for by immunoblotting.

To elucidate mechanisms by which Hsf1 regulates HIF-1□ expression, we studied effects of Hsf1 knockdown on HIF-1 expression in cell culture. Control and shHsf1 MCF7 cells were exposed to hypoxia (1 % oxygen for 16 hours) or hypoxia mimetic DFO (100 μM), and levels of HIF-1□ were monitored by immunoblotting. Knockdown of Hsf1 markedly suppressed accumulation of HIF-1 in response to these stimuli (Fig. 12), similar to suppression of HIF-1accumulation in xenografts

formed by shHsf1 MCF7 cells (Fig. 11). Importantly, Hsf1 knockdown also strongly inhibited secretion of VEGFA, the major growth factor responsible for neovascularization, as well as other targets of HIF-1 CAIX and Glut-1 (Fig. 13, 14).

Fig. 12 Knockdown of Hsf1 in MCF7 cells inhibits HIF-1 accumulation after hypoxia (hyp, 1% 0_2, 16hr), hypoxia mimetic deferoxamine (100 μM, 4 hr), or proteasome inhibitor MG132 (5 μM, 4 hr). Cells were infected with shHsf1 retrovirus, and HIF-1 expression was analyzed by immunoblotting. Hsf1 knockdown also reduces induction of HIF-1a targets CAIX and Glut-1 in MCF7 cells.
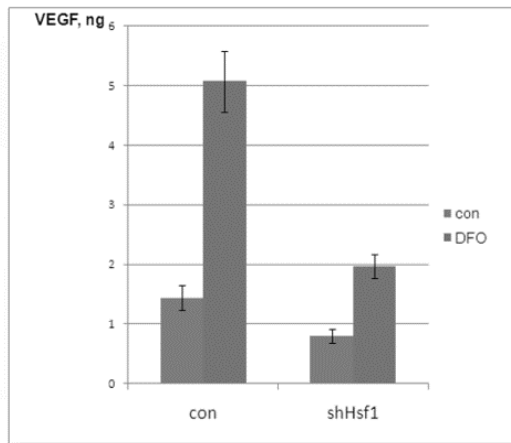
Fig. 13 Hsf1 knockdown reduce induction of HIF-1a target VEGF in MCF7 cells. Cells were infected with Hsf1 retrovirus, treated with DFO for 48 hr, and medium was collected and analyzed by ELISA for VEGFA by Quansys Biosciences.

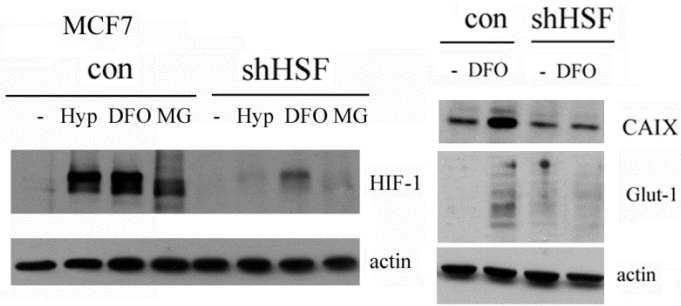Fig. 14 Knockdown of Hsf1 inhibits accumulation of HIF-1 and its targets in MCF10A (left panel) and NeuT-infected MCF10A cells (right panel). Cells were treated with DFO (100 μM, 4 hr) or MG132 (5 μM, 4 hr) and accumulation of HIF-1 and its targets CAIX and Glut-1 was analyzed by immunoblotting.
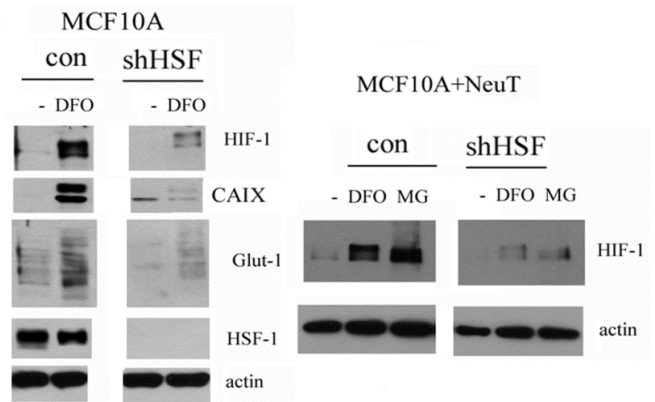
To assess whether effect of Hsf1 knockdown on HIF-1☐ has a general significance, we used other breast cell lines, including normal untransformed cells MCF10A, NeuT-transformed MCF10A, Her2-positive cancer lines MB453 and BT474, and triple-negative Hs578T. In all these cell lines Hsf1 knockdown strongly inhibited accumulation of HIF-1 and its targets CAIX and Glut1 in response to the hypoxia mimetic DFO (Fig. 15).
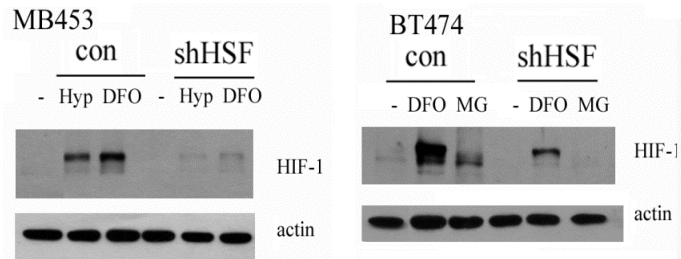
Fig. 15 Her2-positive MB453 (left panel) and BT474 cells (right panel) were infected with Hsf1 retrovirus as in A, treated with hypoxia for 16 hr, or DFO (100 μM, 4 hr), or MG132 (5 μM, 4 hr) and accumulation of HIF-1 was analyzed by immunoblotting.

Fig. 16 Expression of the shRNA-resistant Hsf1 mutant, reverses the effect of shRNA on HIF-1α. Hs578T cells were infected with retrovirus encoding Hsf1* or control retrovirus, and selected. Then Hsf1 was
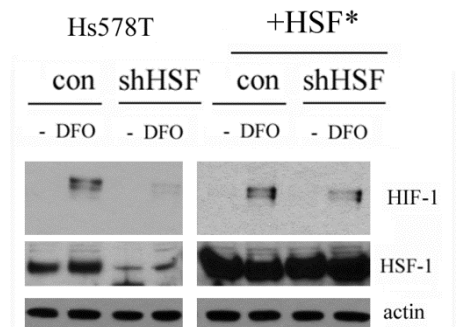
depleted by shRNA, and HIF-1α expression was measured by immunoblotting in naïve cells or following DFO treatments.

This phenomenon was not an off target effect of Hsf1 knockdown, since expression of shRNA-resistant mutant of Hsf1 (Hsf1*) prevented downregulation of HIF-1□□□Therefore, impairment of angiogenesis in NeuT-induced mammary tumors in *hsf1* knockout animals can be associated with inhibition of HIF-1□□expression in tumors. Of note, these effects were not limited to Her2-positive breast cancer cells, since they were seen in Her2-negative, ER positive MCF7 cells and in triple-negative cancer line Hs578T (Fig.16).

Translation factor HuR (ELAV1) mediates effects of Hsf1 on Hif-1.

To Understand the mechanisms of regulation of Hif-1 by Hsf1, we measured Hif-1 protein and mRNA levels, and their degradation rates. Hsf1 affected neither levels of Hif-1 mRNA (Fig. 17A), nor rates of Hif-1 protein degradation (Fig. 17C). On the other hand, we observed strong inhibition of Hif-1 translation in Hsf1-depleted cells, as measured after short pulse of S35-methionine followed by IP (Fig. 17D). There is limited information in the literature about translational regulation of Hif-1. We followed these leads to test which of them is affected by Hsf1 depletion. These experiments show that Hsf1 does not affect activity of mTOR pathway, as measured by phosphorylation of S6 and phospho-4E-BP1 (Fig. 17E). It also did not affect phosphorylation of eIF2a (Fig. 17F). Therefore, we measured effects of Hsf1 on levels of miRNA. Global miRNA analysis by microarray indicated that a set of miRNA are up- or downregulated by Hsf1 (Fig. 17G). Furthermore, many of these miRNA are known to be regulated by hif-1 and hypoxia, further confirming that downregulation of Hif-1 in Hsf1-depleted cells has functional consequences. However, none of these miRNA have binding sites in Hif-1 3'-UTR, and therefore unlikely ot be responsible for the translational regulation of Hif-1.

This research further established that Hif-1 regulation by hsf1 involves the RNA-binding protein HuR. We found that depletion of Hsf1 leads to downregulation of HuR bothe invitro and in the xenograft model (Fig. 18A,B). Furthermore, Depletion of HuR was sufficient to downregulate Hif-1 (Fig. 18C). On the other hand, overexpression of HuR reverse effects of Hsf1 on Hif-1 (Fig. 18D), indicating that Hur mediates the response.

In regulation of HuR, Hsf1 depletion reduced levels of HuR mRNA,but not its rate of decay, indicating that Hsf1 regulates transcription of HuR (Fig. 18E,F,G). Interestingly, more recent publication reported that HuR promoter has Hsf1-binding site (HSE element), and Hsf1 can bind to this site in certain cancer cells (Mendillo et al, 2012). These data suggest that effects of Hsf1 on HuR are direct.

Hur regulates translation of multiple genes beside Hif-1, including genes involved in tumor invasion and metastases. Indeed, some of these genes, e.g. Hif-2, SIRT1, p53, ClnB, were significantly downregulated in Hsf1-depleted cells (Fig. 18H,I,J). Therefore, we have established a novel pathway that contributes to cancer development Hsf1-HuR-Hif-1.
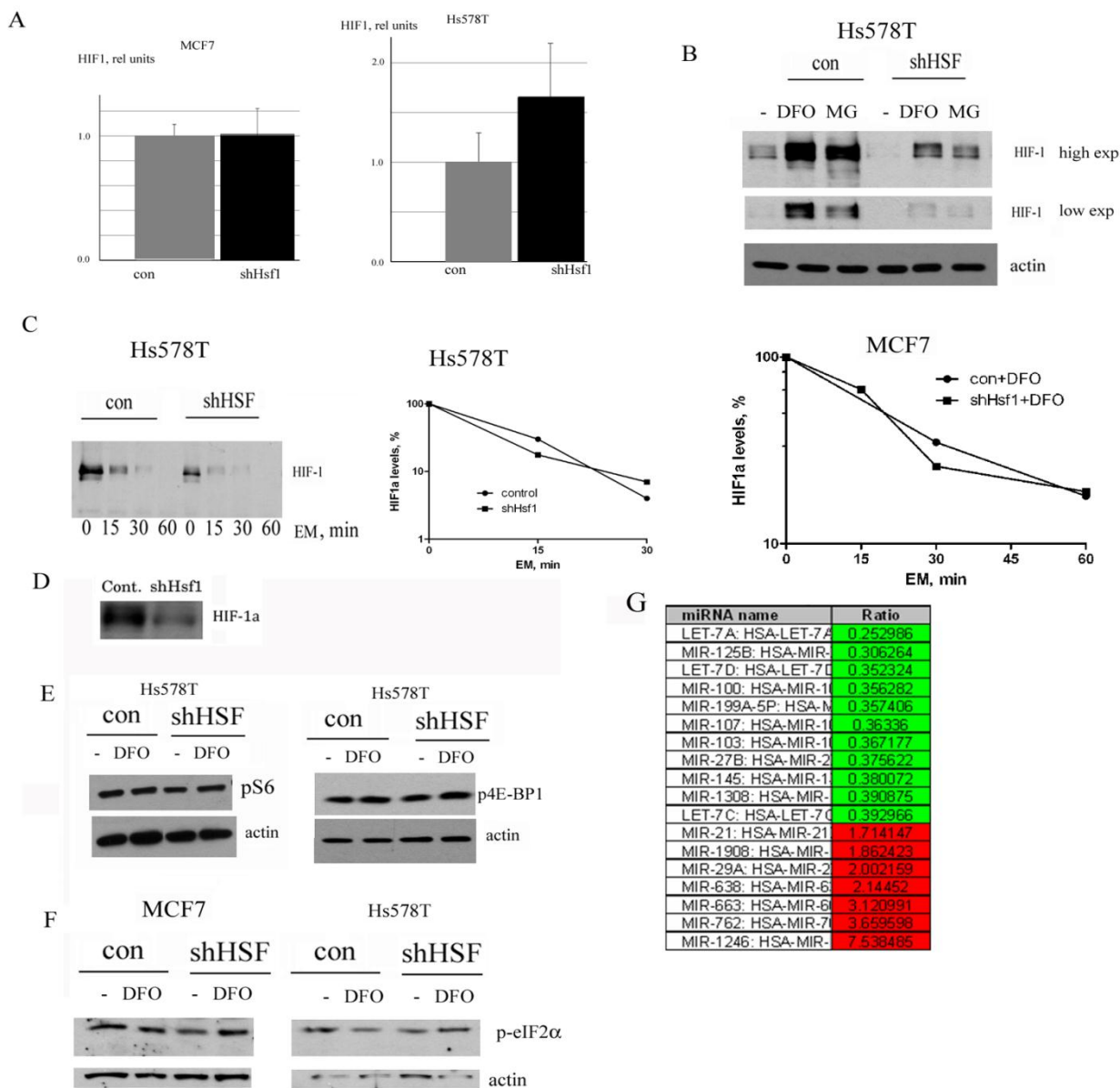
FIG. 17. Effect of Hsf1 knockdown on various levels of HIF-1 expression. A. Effect of Hsf1 knockdown on HIF1α mRNA levels in MCF7 or Hs578T cells; DFO treatment did not change mRNA levels (not shown). RT-qPCR was done as described in Materials and Methods. B. shHsf1 suppresses both basal and DFO (100 μM, 4 hr) or MG-132 (5 μM, 4 hr) -induced levels of HIF-1 in Hs578T cells. C. Knockdown of Hsf1 does not affect stability of HIF-1. Hs578T or MCF7 cells were treated with protein synthesis inhibitor emethine (10 μM), in the absence or presence of DFO (100 μM) for time intervals indicated, and the levels of HIF-1 were determined. Middle panel is quantification of the left panel. D. Hsf1 knockdown reduces translation of HIF-1a. MCF7 cells were labeled with ^{35}S-methoinine for 10 min, and HIF-1 immunoprecipitated, run on SDS PAGE, and exposed to film. The initial material was normalized by TCA-precipitable count (label incorporated into proteins). E. Hsf1 knockdown does not affect activity of mTOR pathway. Activity of mTOR pathway was assayed by antibody to phosphorylated (ser235/236) S6 ribosomal protein, (left panel), or phosphorylated (Ser65) 4E-BP1 (right panel). F. Hsf1 knockdown does not affect phosphorylation of eIF2α, assayed by antibody to phosphorylated (Ser51) eIF2α. G. Effect of shHsf1 knockdown on microRNA profile of Hs578T cells. MicroRNA was isolated and assayed by Miltenyi Biotec. MicroRNAs which are downregulated in shHsf1 cells are shown in green, and upregulated – in red. See text for further explanation.

10

A

Hs578T   MCF7
con   shHsf1   con   shHsf1
HuR   HuR
PTBP1   PTBP1
actin   actin

B
#1   #2
con shHsf con shHsf
HuR
PTBP1
actin

C
Hs578T
con   shHuR
- DFO MG   - DFO MG
HIF-1
HuR
actin

MCF7
con   shHuR
- DFO   - DFO
HIF-1
HuR
actin

D
Hs578T   + HuR
con   shHsf1   con   shHsf1
- DFO - DFO   - DFO - DFO
HIF-1
Hsf1
HuR
actin

MCF7   + HuR
con   shHsf1   con   shHsf1
- DFO - DFO   - DFO - DFO
HIF-1
HuR
actin

E
HuR
Relative mRNA
1.2
1
0.8
0.6
0.4
0.2
0
con shHsf1   con shHsf1
Hs578T   MCF7

F
HuR   MCF7
Relative mRNA
100%

10%
0   1.5   3
Act D, hr
Control
shHSF1

G
Relative mRNA
9
8
7
6
5
4
3
2
1
0
p<.05
■ WT (n=3)
■ Hsf1 -/- (n=2)
HuR

WT1 WT2 KO1 KO2
HuR
Actin
1   .61 .20 .35

H
Hs578T
con   shHSF
- DFO - DFO
HIF-2
actin

MCF7
con   shHSF
- DFO MG - DFO MG
HIF-2
actin

I
Hs578T
con   shHSF
- DFO MG - DFO MG
Sirt1
actin

MCF7
con   shHsf1
- DFO - DFO
Sirt1
actin

J
Hs578T
con   shHsf1
- DFO - DFO
p53
actin

MCF7
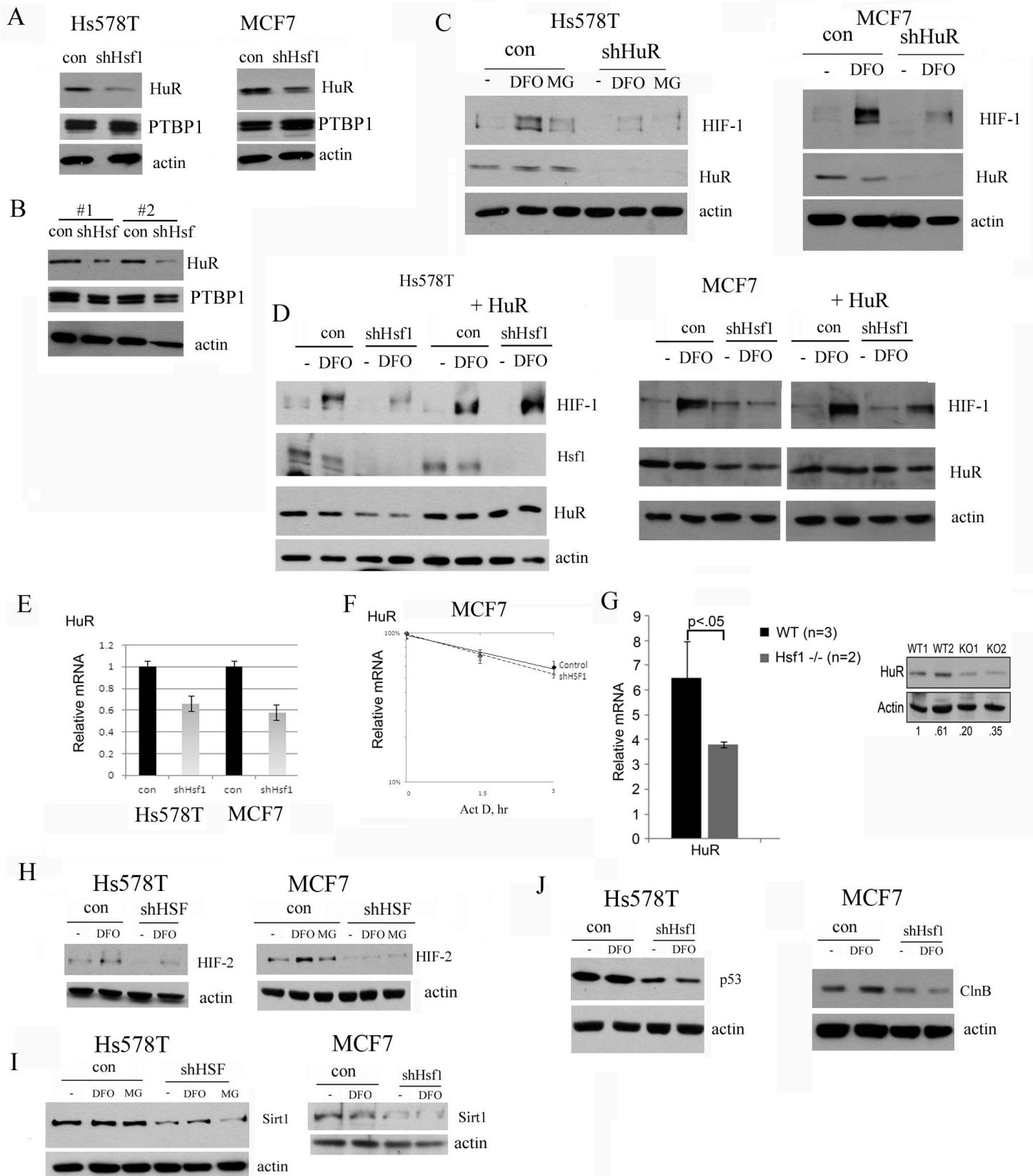con   shHsf1
- DFO - DFO
ClnB
actin

FIG. 18. Suppression of HIF-1 accumulation by shHsf1 is associated with HuR downregulation.

A. Hsf1 knockdown decreases HuR, but not PTBP1 levels in Hs578T (left panel) and MCF7 cells (right panel). B. Hsf1 knockdown decreases HuR, but not PTBP1 levels in MCF7 xenografts (see Fig. 3B-D). C. Knockdown of HuR suppresses HIF-1 accumulation in Hs578T (left panel) and MCF7 cells (right panel). Cells were infected with shHuR retrovirus, selected and treated with DFO (100 μM) or MG-132 (5 μM) for 4 hr. D. HuR overexpression prevents inhibition of HIF-1 accumulation by Hsf1 knockdown. Hs578T and MCF7 cells were first infected with HuR retrovirus, and selected. HuR-expressing cells were infected with shHsf1 retrovirus as described in Materials and Methods, and treated with 100 μM of DFO for 4 hr. E. Hsf1 knockdown leads to reduction of HuR mRNA levels in Hs579T and MCF7 cells. F. Hsf1 knockdown does not affect stability of HuR mRNA. Levels of HuR mRNA were measured by qRT-PCR after inhibition of transcription by Actinomycin at the indicated time points. G. Levels of HuR mRNA and protein were assessed in liver of control and hsf1 KO mice. H, I, J. Hs578T and MCF7 cells were infected with shHsf1 retrovirus as in Fig. 4A, 5B, treated with DFO (100 μM), or MG-132 (5 μM) for 4 hr, and the levels of HIF-2α (H), Sirt1 (I), p53 (mutant) (J), or cyclin B (J) were assayed by immunoblotting.

Our further investigations revealed that Hsf1-HuR-Sirt1 pathway forms a positive feedback loop, which enhances chronic inflammation and plays an important role in maintenance of senescence (Kim et al, 2012).

Task 4.

To test whether NZ28 inhibits tumor angiogenesis in xenografts of Her2-expressing MCF10A cells.

In accordance to the task, we have established tumor xenografts with Her2-expressing MCF10A cells. When tumor volumes reached about 150mm^3, 50mg/kg NZ28 was administered daily by IP injections with water solution over 7 days. As controls we used bolus-injected animals. On day 8 mice were sacrificed, and tumors collected and frozen. Expression of Hif1, Glut1, carbonic anhydrase IX, angiogenesis and necrosis were monitored.

NZ28 had relatively minor effect on the tumor growth, reducing it by less than 30%. Under these conditions, we did not detect significant effects on tumor vasculature, and expression of Hif1. These small effects were probably due to the rapid metabolism of NZ28. In light of these data, we decided not to proceed to Task 5, since it was dependent on the success of Task 4.

Key Research Accomplishments:

- Demonstrated that Hsf1 knockout inhibits Her2/NeuT-induced hyperplasia of mammary tissue.
- Demonstrated that Hsf1 knockout inhibits Her2/NeuT-induced tumor emergence.
- Demonstrated that Hsf1 knockout inhibits growth of Her2/NeuT-induced tumors.
- Demonstrated that Hsf1 knockout inhibits angiogenesis in Her2/NeuT-induced tumors.
- Developed a xenograft model that recapitulates effects of hsf1 on tumor growth.
- Demonstrated that in this xenograph model Hsf1 controls angiogenesis.
- Demonstrated that Hsf1 controls the angiogenesis transcription factor HIF-1 and its targets in xenografts and culture of breast cancer cells.
- Demonstrated that Hsf1 regulates Hif-1 at the level of translation.
- Demonstrated that the translational regulator RNA binding protein HuR mediates effects of Hsf1 on Hif-1.
- Demonstrated that via HuR Hsf1 regulates a wide range of pathways that facilitate tumorigenesis, including invasion and metastases.

- Established a positive feedback loop Hsf1-HuR-Sirt1 that is responsible for the maintenance of senescence and chronic inflammation.

Reportable outcomes:

Two papers have been published:

1. Gabai VL, Meng L, Kim G, Mills TA, Benjamin IJ, Sherman MY (2012) Heat shock transcription factor Hsf1 is involved in tumor progression via regulation of hypoxia-inducible factor 1 and RNA-binding protein HuR. *Mol Cell Biol* **32**(5)**:** 929-940

2. Kim G, Meriin AB, Gabai VL, Christians E, Benjamin I, Wilson A, Wolozin B, Sherman MY (2012) The heat shock transcription factor Hsf1 is downregulated in DNA damage-associated senescence, contributing to the maintenance of senescence phenotype. *Aging Cell* **11**(4)**:** 617-627

An application for the Idea Expansion Award based on results of this Idea Award has been submitted.

List of Personnel Who Received Pay from the Research Effort:

Michael Sherman, Ph.D. – Principal Investigator
Vladimir Gabai, Ph.D. – Faculty
Le Meng – Graduate Student
Teresa Mills – Graduate Student

Conclusion:

This study demonstrates that Hsf1 controls development of Her2-positive cancer both at the stage of initiation, via control of the oncogene-induced senescence, and progression, via regulation of tumor angiogenesis. It also dissects the mechanism of effects of Hsf1 on tumor angiogenesis, and demonstrates that Hsf1 regulates expression of the major angiogenesis factor HIF-1, and this regulation involves the translation regulator HuR. This program provides rationale for development of Hsf1 inhibitors that can inhibit multiple pathways in tumor initiation and progression. It also establishes a simple xenograft model that can be used for anti-Hsf1drug testing.

References

Dai C, Whitesell L, Rogers AB, Lindquist S (2007) Heat shock factor 1 is a powerful multifaceted modifier of carcinogenesis. *Cell* **130**(6)**:** 1005-1018

Gabai VL, Meng L, Kim G, Mills TA, Benjamin IJ, Sherman MY (2012) Heat shock transcription factor Hsf1 is involved in tumor progression via regulation of hypoxia-inducible factor 1 and RNA-binding protein HuR. *Mol Cell Biol* **32**(5)**:** 929-940

Gordan JD, Simon MC (2007) Hypoxia-inducible factors: central regulators of the tumor phenotype. *Curr Opin Genet Dev* **17**(1)**:** 71-77

Guy CT, Webster MA, Schaller M, Parsons TJ, Cardiff RD, Muller WJ (1992) Expression of the neu protooncogene in the mammary epithelium of transgenic mice induces metastatic disease. *Proc Natl Acad Sci U S A* **89**(22)**:** 10578-10582

Kim G, Meriin AB, Gabai VL, Christians E, Benjamin I, Wilson A, Wolozin B, Sherman MY (2012) The heat shock transcription factor Hsf1 is downregulated in DNA damage-associated senescence, contributing to the maintenance of senescence phenotype. *Aging Cell* **11**(4)**:** 617-627

Mendillo ML, Santagata S, Koeva M, Bell GW, Hu R, Tamimi RM, Fraenkel E, Ince TA, Whitesell L, Lindquist S (2012) HSF1 drives a transcriptional program distinct from heat shock to support highly malignant human cancers. *Cell* **150**(3)**:** 549-562

Meng L, Gabai VL, Sherman MY (2010) Heat-shock transcription factor HSF1 has a critical role in human epidermal growth factor receptor-2-induced cellular transformation and tumorigenesis. *Oncogene* **29**(37)**:** 5204-5213

Meng L, Hunt C, Yaglom JA, Gabai VL, Sherman MY (2011) Heat shock protein Hsp72 plays an essential role in Her2-induced mammary tumorigenesis. *Oncogene* **30**(25)**:** 2836-2845

Min JN, Huang L, Zimonjic DB, Moskophidis D, Mivechi NF (2007) Selective suppression of lymphomas by functional loss of Hsf1 in a p53-deficient mouse model for spontaneous tumors. *Oncogene* **26**(35)**:** 5086-5097

Muller WJ, Arteaga CL, Muthuswamy SK, Siegel PM, Webster MA, Cardiff RD, Meise KS, Li F, Halter SA, Coffey RJ (1996) Synergistic interaction of the Neu proto-oncogene product and transforming growth factor alpha in the mammary epithelium of transgenic mice. *Mol Cell Biol* **16**(10)**:** 5726-5736

Santagata S, Hu R, Lin NU, Mendillo ML, Collins LC, Hankinson SE, Schnitt SJ, Whitesell L, Tamimi RM, Lindquist S, Ince TA (2012) High levels of nuclear heat-shock factor 1 (HSF1) are associated with poor prognosis in breast cancer. *Proc Natl Acad Sci U S A* **108**(45)**:** 18378-18383

Semenza GL (2009) Defining the role of hypoxia-inducible factor 1 in cancer biology and therapeutics. *Oncogene* **29**(5)**:** 625-634

Heat Shock Transcription Factor Hsf1 Is Involved in Tumor Progression via Regulation of Hypoxia-Inducible Factor 1 and RNA-Binding Protein HuR

Vladimir L. Gabai, Le Meng, Geunwon Kim, Teresa A. Mills, Ivor J. Benjamin and Michael Y. Sherman

	Updated information and services can be found at: http://mcb.asm.org/content/32/5/929
	These include:
REFERENCES	This article cites 37 articles, 16 of which can be accessed free at: http://mcb.asm.org/content/32/5/929#ref-list-1
CONTENT ALERTS	Receive: RSS Feeds, eTOCs, free email alerts (when new articles cite this article), more»

Heat Shock Transcription Factor Hsf1 Is Involved in Tumor Progression via Regulation of Hypoxia-Inducible Factor 1 and RNA-Binding Protein HuR

Vladimir L. Gabai,[a] Le Meng,[a] Geunwon Kim,[a] Teresa A. Mills,[a] Ivor J. Benjamin,[b] and Michael Y. Sherman[a]

Department of Biochemistry, Boston University Medical School, Boston, Massachusetts, USA,[a] and Center for Cardiovascular Translational Biomedicine, Division of Cardiology, Department of Internal Medicine, Department of Biochemistry, University of Utah, School of Medicine, Salt Lake City, Utah, USA[b]

Previously we demonstrated that the heat shock transcription factor Hsf1 is indispensable for transformation of mammary epithelial cells by the Her2 oncogene. Since Hsf1 affects oncogene-induced senescence (OIS), these findings suggest that Hsf1 affects tumor initiation when OIS plays a role. Indeed, here we report that Hsf1 knockout suppressed mammary hyperplasia in Her2-expressing mice and reduced tumor emergence. On the other hand, Hsf1 expression increases with advanced breast cancer, indicating that there is an additional role of Hsf1 in tumor progression. We studied rare tumors that developed in Hsf1-knockout mice and found that these tumors grew slower than tumors in control animals and showed suppressed angiogenesis. Similarly, in the xenograft model, knockdown of Hsf1 suppressed angiogenesis, which was associated with suppression of the HIF-1 pathway. Suppression of HIF-1 was at the level of translation due to downregulation of the RNA-binding protein HuR. Importantly, besides HIF-1, HuR controls translation of other major regulators of cancer progression, many of which were suppressed in Hsf1-knockdown cells. Therefore, in addition to OIS, Hsf1 regulates the HuR–HIF-1 pathway, thus affecting both cancer initiation and progression.

The heat shock transcription factor 1 (Hsf1) is the major regulator of the heat shock response (33) that is involved in protection of cells and organisms from heat, ischemia, inflammation, oxidative stress, and some other noxious conditions. Among proteins activated by Hsf1, the major defensive function is attributed to heat shock proteins (Hsps) such as Hsp70, Hsp90, and Hsp27, though besides Hsps, Hsf1 regulates hundreds of other targets (32). Initially, Hsps were described as molecular chaperones that prevent and repair protein damage, but later it became clear that their functions go beyond protein folding or degradation, since Hsps also play a distinct and essential role in cell signaling, for example, in suppression of apoptotic pathways or mitogen-activated protein (MAP) signaling cascades (4, 15).

Numerous studies indicate that Hsf1 and Hsps are overexpressed in a variety of human tumors (11). Furthermore, it was recently demonstrated that Hsf1 is critical for tumorigenesis by certain oncogenes. Indeed, it was demonstrated that *Hsf1* knockout (KO) suppresses lymphoma development in *p53*-knockout mice (30). Furthermore, *hsf1* knockout dramatically delayed overall development of tumors and increased survival of *p53*-knock-in mutant (R172H) mice (13). Similarly, *Hsf1* deficiency drastically postponed RAS-induced chemical skin carcinogenesis and increased survival of mice from 30% to 90% (13).

We have recently demonstrated that the major Hsf1 target Hsp72 (HSPA1, or inducible Hsp70) plays an essential role in Her2 (NeuT)-induced tumorigenesis in mice (29). This mouse tumor model is widely used to study mechanisms of human breast cancer since it recapitulates initiation and progression of Her2-positive breast cancer, occurring in 15 to 25% of patients. Interestingly, activation of Her2 signaling by heregulin or Her2 overexpression can activate Hsf1 (22, 28).

Importantly, Hsf1 and Hsp72 are essential not only for initial transformation but also for maintaining viability and growth of a variety of fully transformed cells (13, 28, 29). On the other hand,

Hsf1 and Hsp72 are dispensable for viability and growth of nontransformed human cells and whole animals (13, 20, 28, 29). The specific dependence of cancer cells on Hsf1 and chaperones was named "nononcogene addiction" (35).

In searching for the mechanism of tumor addiction to Hsf1 and Hsp72, we have found that Hsf1 and Hsp72 play an important role in evasion of oncogene-induced senescence (OIS) (16, 28, 29), which is critical for early stages of neoplastic transformation. Cellular senescence was originally described as a limit to the number of divisions that a normal cell can undergo. Senescence can be triggered by telomere shortening or stressful treatments and is associated with activation of p53 and accumulation of the cell cycle inhibitors p21 and/or p16 (5). Although tumor cells are immortal and divide indefinitely, they often retain functional senescence programs and can become senescent in response to various DNA-damaging drugs and radiation (9), which is especially relevant to solid tumors of epithelial origin. Importantly, cell senescence can be triggered upon activation of oncogenes, e.g., Ras or Raf (6, 26), which was observed in various systems, including human precancerous tissues. Therefore, a novel concept has emerged that oncogene-induced senescence (OIS) represents the major block on the path toward the neoplastic transformation, and cells in emerging tumors must acquire adaptations/mutations that allow the senescence bypass (8). We have found that Hsf1 and

Hsp72 are critically involved in prevention of the oncogene-induced senescence caused by PIK3CA, Ras, and Her2 oncogenes. These effects were associated with suppression of accumulation of p21 and decrease in survivin levels (16, 28, 29).

The finding of the role of Hsf1 and Hsp72 in OIS suggests that these factors control early stages of tumorigenesis. This idea is in line with our data with *Hsp72*-knockout mice, which show dramatic suppression of early hyperplasia induced by the Her2 oncogene and development of senescence of epithelial cells in ducts (29). On the other hand, there are multiple reports that expression levels of Hsf1 and Hsp72 closely correlate with tumor grade, suggesting that these proteins could also be involved in later stages of tumor progression, including invasion and metastasis (see reference 11 for a review).

Here we addressed the possibility of involvement of Hsf1 in later stages of tumor progression by investigating why rare tumors that emerge in *Her2*-expressing *Hsf1*-knockout animals grow slower than tumors in control mice. We found that Hsf1 plays an additional important function in tumorigenesis by affecting hypoxia-inducible factor 1 (HIF-1)-dependent angiogenesis. HIF-1 is a master regulator not only of genes that control tumor neovascularization but also of those that control glycolysis, pH regulation, invasion, and metastasis (18, 34).

Here, we found that Hsf1 controls HIF-1 via the mRNA-binding protein HuR, which in turn controls an even wider set of cancer-related genes, including genes that regulate cell cycle, apoptosis, invasion, and angiogenesis. Therefore, besides being necessary for tumor initiation by blocking oncogene-induced senescence, Hsf1 also plays a critical role in tumor progression by regulating multiple genes controlled by HIF-1 and HuR.

MATERIALS AND METHODS

Animals. Animal maintenance and experiments were conducted in compliance with IACUC guidelines. MMTVneu$^{+/+}$ mice (FVB/N; Jackson Laboratory) were crossed with wild-type (WT) mice or hsf1$^{-/-}$ mice (129/BALB) (27, 36) to generate WT-MMTVneu$^{+/-}$, hsf1$^{+/-}$ MMTVneu$^{+/-}$, and hsf1$^{-/-}$ MMTVneu$^{+/-}$ mice. Mice were sacrificed at 3 months of age to study mammary gland hyperplasia or kept to monitor tumor development.

Xenografts. For establishing tumor xenografts, MCF7 cells were trypsinized and mixed at a 1:1 ratio with Matrigel, and 1 million cells were injected subcutaneously into either left (control) or right (shHsf1-knockdown) flanks of 6-week-old female NCR nude mice (Taconic). Tumor growth was measured weekly using caliper and calculated according to the formula $L \times W^2 \times \pi/6$, where L is length and W is width.

Angiogenesis. Tumors were removed from animals when they reached approximately 1 cm^3 in WT mice or control xenografts; corresponding tumors in knockout (KO) animals or shHsf1 xenografts were smaller. Tumors were fixed with formalin, and CD31 staining and analysis were performed by Premier Lab using Aperio ImageScope software.

Cell cultures and reagents. MCF10A cells were cultured in Dulbecco's modified Eagle's medium (DMEM)–F-12 medium supplemented with 5% horse serum, 20 ng/ml epidermal growth factor (EGF), 0.5 μg/ml hydrocortisone, 10 μg/ml human insulin, and 100 ng/ml cholera toxin. HEK293T cells were from ATCC and were cultivated in DMEM supplemented with 10% heat-inactivated fetal bovine serum (FBS). MDA-MB453 cells were cultured in Leibovitz's L-15 medium with 10% FBS. Other cell lines were grown in DMEM with 10% FBS. All media contained penicillin and streptomycin (500 units per ml).

Retroviral vectors and infection. RNAi-Ready pSIREN-RetroQ vector from the BD Biosciences retroviral delivery system was used for knockdown of HSF1. The sequence of the human HSF1 gene was selected as reported before (5'-TATGGACTCCAACCTGGATAA-3') (37). shHuR

lentivirus was purchased from Open Biosystems (Huntsville, AL). For HuR overexpression, HuR lentiviral open reading frames (ORFs) were purchased from Open Biosystems and HuR sequence was cloned by PCR and inserted into pQCXIN vector (BD Biosciences) at AgeI and PacI sites.

Retroviruses were produced as reported before (16). Briefly, HEK293T cells were cotransfected with plasmids expressing retroviral proteins Gag-Pol, vesicular stomatitis virus glycoprotein (VSV-G) pseudotype, and enhanced green fluorescent protein (EGFP) or our constructs using Lipofectamine 2000 (Invitrogen). Lentiviruses were produced by transfection of 293T cells with plasmids psPAX2, pMD2.G, and our constructs. Forty-eight hours after transfection, supernatants containing the retroviral particles were collected and frozen at −80°C until use. Cells were infected with diluted supernatant in the presence of 10 μg/ml Polybrene overnight and were selected with puromycin (0.75 μg/ml) 48 h after infection. Retroviral or lentiviral vectors expressing EGFP were used as an infection efficiency indicator: usually ~90% of cells were fluorescent 2 days after infection.

qRT-PCR. For total RNA preparation and quantitative real-time PCR (qRT-PCR), tissues from mice were harvested and preserved in RNAlater reagent (Qiagen). Total RNAs from tissues or cells were isolated using the RNeasy minikit (Qiagen) and reverse transcribed with the RetroScript kit (Ambion), according to the manufacturer's instructions. qRT-PCR was performed using SYBR green Rox Master Mix (Qiagen).

Primer sequences used in qRT-PCR are as follows: human HuR, For, 5'-CAGGAAACGCCTCCTCCGGC-3', and Rev, 5'-ACGGCACCAAAC GGCCCAAA-3'; human glyceraldehyde-3-phosphate dehydrogenase (GAPDH), For, 5'-GGCCTCCAAGGAGTAAGACC-3', and Rev, 5'-AG GGGAGAGATTCAGTGTGGTG-3'; mouse HuR, For, 5'-GGATGACAT TGGGAGAACGAAT-3', and Rev, 5'-TGTCCTGCTACTTTATCCCGA A-3'; mouse GAPDH, For, 5'-AAATTCAACGGCACAGTCAAGG-3', and Rev, 5'-GCCTCACCCCATTTGATGTTAGT-3'; human HIF-1, 5'-A AAGAGGTGGGATATGTCTGGGTT, and Rev, 5'-TGCTGAATAATAC CACTCACAACGT.

mRNA stability study. HuR mRNA half-life ($t_{1/2}$) was measured in control (CT) and Hsf1-depleted (shHsf1) cells by incubation with 5 μg/ml of actinomycin D and collection of RNA after 1.5 h and 3 h. HuR and GAPDH mRNAs were measured by qRT-PCR and normalized by GAPDH mRNA. Data are represented as percentages of HuR mRNA measured at time zero (prior to adding actinomycin D), on a semilogarithmic scale.

Immunoblotting and translation analysis. Cells were washed twice with phosphate-buffered saline (PBS) and lysed in lysis buffer (40 mM HEPES, pH 7.5, 50 mM KCl, 1% Triton X-100, 1 mM Na$_3$VO$_4$, 50 mM glycerophosphate, 50 mM NaF, 5 mM EDTA, 5 mM EGTA, 1 mM phenylmethylsulfonyl fluoride, 1 mM benzamidine, and 5 μg/ml each leupeptin, pepstatin A, and aprotinin). Mouse tissues or xenografted tumor was snap-frozen in liquid nitrogen and then homogenized in the same buffer and centrifuged for 5 min at 1,000 × g, and supernatants were collected. Protein concentration of the lysates was measured with the Bio-Rad protein assay reagent, after which they were diluted with lysis buffer to achieve equal protein concentrations. For measuring HIF-1α translation, MCF7 cells were labeled in 35-mm plates with EasyTag [^{35}S]methionine (Perkin-Elmer) in methionine-free medium for 10 min. Lysates were prepared, and HIF-1α was immunoprecipitated.

Antibodies used for this study were anti-pS6, anti-p4E-BP1, p-eIF2α, and anti-Sirt1 from Cell Signaling; anti-HIF-1α, anti-p21, and anti-cyclin B from BD PharMingen; anti-HuR, anti-p53, and antisurvivin from Santa Cruz; anti-HSF1 from Stressgen; anti-HIF-2α, anti-CA9, and anti-Glut-1 from Novus Biolab; anti-PTBP1 from BioLegend; and anti-β-actin from Sigma.

RESULTS

Hsf1 knockout suppresses Her2-induced hyperplasia and tumor development. We have previously found that knockdown of Hsf1 in MCF10A human mammary epithelial cells prevents neo-
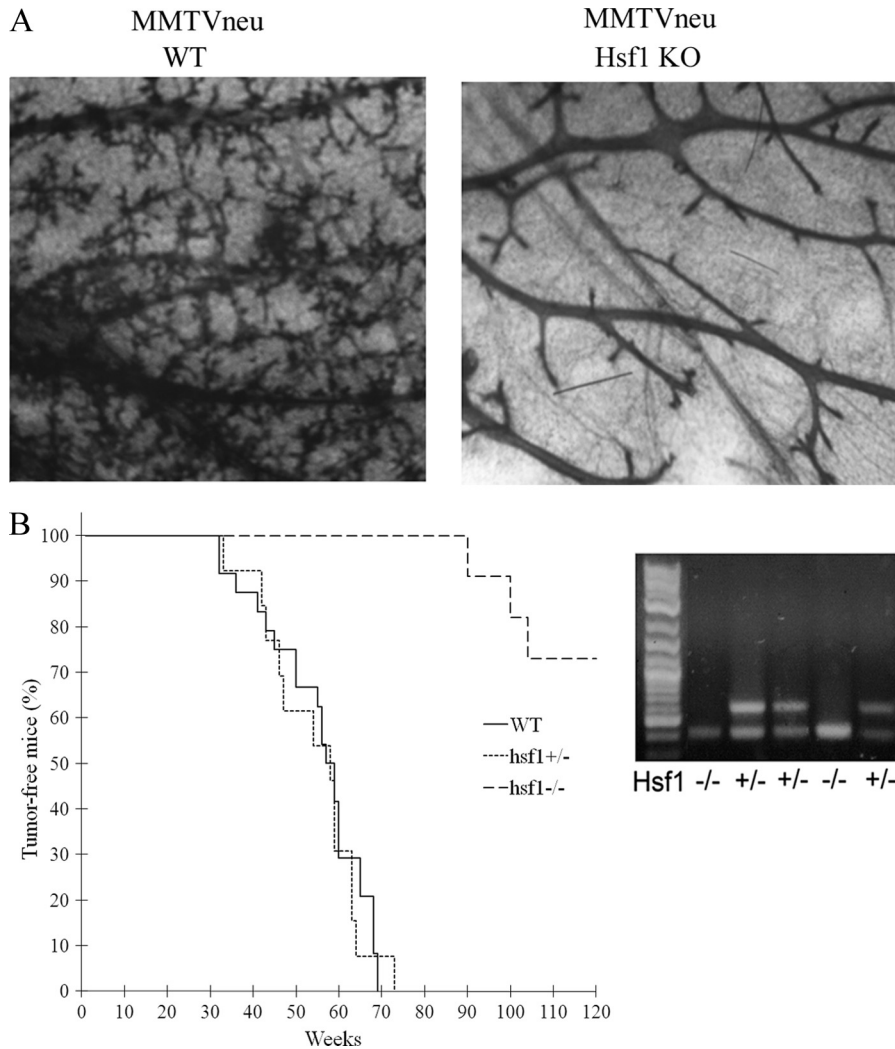
FIG 1 Knockout of Hsf1 blocks NeuT-induced mammary duct and alveolar branching and delays tumor emergence. (A) WT-*MMTVneu*+ and *hsf1*−/− *MMTVneu*+ mice were sacrificed at 3 months of age, and whole mounts of their mammary glands were observed after application of Carnoy's fixative and staining with carmine. (B) Emergence of NeuT-induced tumors in WT-*MMTVneu*+ (*n* = 16), heterozygous *hsf1*+/− *MMTVneu*+ (*n* = 13), and *hsf1*−/− *MMTVneu*+ (*n* = 11) animals. Lack of Hsf1 in the knockout animals is shown by PCR.

plastic transformation by the Her2 oncogene. Indeed, while expression of Her2 in control MCF10A cells facilitated focus formation in culture and tumor appearance in nude mice, expression of this oncogene in *Hsf1* knockdown MCF10A cells led to growth arrest and OIS, and tumors could not form in nude mice (28). To further dissect where in the tumorigenic process Hsf1 exerts its activity, here we used the transgenic animal model. Accordingly, we crossed *Hsf1*-knockout animals with mice expressing Her2/NeuT (a rodent homolog of Her2 carrying an activating mutation) under the control of the mouse mammary tumor virus (MMTV) promoter (MMTVneu) (19) to generate WT-*MMTVneu*+, *hsf1*+/− *MMTVneu*+, and *hsf1*−/− *MMTVneu*+ mice. Because of the mixed background, in the experiments with transgenic animals we used WT littermates as controls for the knockouts.

To investigate the role of Hsf1 in Her2-induced hyperplasia, mammary glands were taken from 3-month-old virgin mice to evaluate duct branching. Expression of Her2 in WT-*MMTVneu*+

mammary gland led to high density of ducts and extensive alveolar branching, as reported previously (31). Importantly, in *hsf1*−/− *MMTVneu*+ animals there was a low duct density and almost no alveolar branching (Fig. 1A). Therefore, *Hsf1* KO prevented Her2-induced tissue hyperplasia, possibly by aggravating senescence, similar to what we have found recently with NeuT-induced mammary tumors in the Hsp72-knockout mouse model (29).

To address whether Hsf1 KO suppresses NeuT-dependent tumorigenesis *in vivo*, we analyzed effects of Hsf1 knockout on NeuT-induced tumor development. Tumor incidences were similar between heterozygous *hsf1*+/− *MMTVneu*+ and WT-*MMTVneu*+ mice (median tumor appearance in this strain was about 55 weeks), indicating that one copy of the *Hsf1* gene is sufficient to support mammary tumor emergence induced by Her2/NeuT (Fig. 1B). In contrast, the absence of Hsf1 in homozygous knockout animals markedly inhibited mammary tumor development (Fig. 1B). Indeed, tumor emergence was strongly delayed, and only three tumors of 11 animals appeared (Fig. 1B).

Therefore, this model of Her2-positive breast cancer establishes that Hsf1 is critical for tumor initiation and hyperplasia.

Hsf1 knockdown suppresses tumor growth and angiogenesis. To investigate whether Hsf1 has additional effects on later stages of tumor development, we measured growth rates of rare tumors that emerge in *Hsf1*-KO animals compared to control mice. Indeed, these tumors grew significantly slower than in control animals (Fig. 2A), indicating that Hsf1 may be required not only for NeuT-induced initial transformation but for tumor progression as well.

Since among the major factors limiting growth of solid tumors *in vivo* is neovascularization, we excised tumors from control and knockout animals, prepared slides, and immunostained them with a marker of angiogenesis (endothelial cells), CD31. We observed that although the numbers of blood vessels were similar in WT and KO animals (not shown), the mean vessel area in tumors from Hsf1-knockout animals was almost twice as small as in wild-type animals (Fig. 2B and C), indicating that the vessels were underdeveloped. These data were in line with microarray data deposited in Oncomine, a human cancer gene array database (www.oncomine.org), where elevated levels of Hsf1 in human breast cancer correlated with grade, metastasis, and poor prognosis (Fig. 2D), also suggesting that Hsf1 is involved in tumor progression.

Since in the transgenic mouse model Hsf1 is lacking both in mammary tumor and in surrounding stroma, to understand mechanisms by which Hsf1 can regulate angiogenesis, we decided to switch from NeuT-induced mouse mammary tumors to a simpler system, i.e., xenograft with human breast cancer cells following Hsf1 knockdown. In this system, Hsf1 can be downregulated specifically in human tumor cells but remain expressed normally in surrounding mouse stroma. As we reported previously, growth of many cancer cell lines (e.g., NeuT-expressing MCF10A cells or MDA-MB453 cells) is dependent on Hsf1, since Hsf1 knockdown causes senescence due to accumulation of p21 and downregulation of the mitotic and antiapoptotic protein survivin (28). Therefore, these cell lines cannot propagate even *in vitro* upon depletion of Hsf1, and accordingly, effects of Hsf1 on angiogenesis cannot be studied in this system. To avoid this problem, we screened several breast tumor cell lines and found that *Hsf1* knockdown does not decrease survivin levels and does not increase p21 levels in MCF7 human breast carcinoma (Fig. 3A). Accordingly, growth of these cells *in vitro* was not significantly affected by *Hsf1* knockdown (Fig. 3A).

Therefore, we have chosen MCF7 cells to assess the effect of Hsf1 knockdown on tumor angiogenesis and growth *in vivo* in the xenograft model. MCF7 cells were infected with retroviral vector expressing shHsf1 as described before and selected with puromycin for 5 days. To avoid possible variations of host factor(s) which could affect tumor growth, control cells were injected in right flanks and shHsf1-knockdown cells were injected in left flanks of the same animals and their growth was monitored by caliper. Tumors emerged at the sites of injection of both control and Hsf1-depleted cells on day 9 after inoculation (Fig. 3B). Importantly, after tumor emergence, tumors formed by control MCF7 cells grew rapidly, while tumors formed by the *Hsf1* knockdown ceased to grow soon after emergence (Fig. 3B). The strong inhibitory effect of *Hsf1* knockdown on growth of MCF7 cells in xenografts was in sharp contrast with cell culture, where Hsf1 knockdown practically did not affect the growth rate (Fig. 3A). We have isolated tumors, stained them for CD31 as described above, and

found that, similar to NeuT-induced mammary tumors in *Hsf1*-KO mice, Hsf1 knockdown markedly decreased mean vessel area in MCF7 human breast cancer xenografts (Fig. 3C) (of note, there was no significant difference in the number of vessels). These data indicate that the xenograft model recapitulates effects of Hsf1 seen in the transgenic model and suggest that control of tumor angiogenesis may represent an important factor regulated by Hsf1.

Hsf1 controls expression of HIF-1. Hypoxia-inducible factor 1 (HIF-1) is considered to be the major regulator of tumor angiogenesis (18, 34), and therefore, we assessed its expression in xenografts formed by MCF7 cells with Hsf1 knockdown. We found high levels of HIF-1α in control tumors (which indicated hypoxic conditions in xenografts), but in tumors with *Hsf1* knockdown, there were much lower levels of HIF-1α (Fig. 3D). Similarly, in *Hsf1* knockdown tumors we observed downregulation of HIF-1α target CAIX (carbonic anhydrase 9) (Fig. 3D). Accordingly, Hsf1 appears to control angiogenesis in xenografts via regulating accumulation of HIF-1α.

To elucidate mechanisms by which Hsf1 regulates HIF-1α expression, we studied effects of Hsf1 knockdown on HIF-1α expression in cell culture. Control and shHsf1 MCF7 cells were exposed to hypoxia (1% oxygen for 16 h) or the hypoxia mimetic deferoxamine (DFO) (100 μM), and levels of HIF-1α were monitored by immunoblotting. Knockdown of *Hsf1* markedly suppressed accumulation of HIF-1α in response to these stimuli (Fig. 4A), similar to suppression of HIF-1α accumulation in xenografts formed by shHsf1 MCF7 cells (Fig. 3D). Importantly, Hsf1 knockdown also strongly inhibited secretion of vascular endothelial growth factor (VEGF), the major growth factor responsible for neovascularization, as well as other targets of HIF-1α, CAIX, and Glut-1 (Fig. 4B).

To assess whether the effect of *Hsf1* knockdown on HIF-1α has a general significance, we used other breast cell lines, including normal untransformed cell line MCF10A, NeuT-transformed MCF10A, Her2-positive cancer lines MB453 and BT474, and triple-negative Hs578T. In all these cell lines, *Hsf1* knockdown strongly inhibited accumulation of HIF-1α and its targets CAIX and Glut-1 in response to the hypoxia mimetic DFO (Fig. 4C to E and data not shown). This phenomenon was not an off-target effect of *Hsf1* knockdown, since expression of a short hairpin RNA (shRNA)-resistant mutant of *Hsf1* (*Hsf1**) prevented downregulation of HIF-1α. Therefore, impairment of angiogenesis in NeuT-induced mammary tumors in *hsf1*-knockout animals can be associated with inhibition of HIF-1α expression in tumors. Of note, these effects were not limited to Her2-positive breast cancer cells, since they were seen in Her2-negative, estrogen receptor (ER)-positive MCF7 cells and in triple-negative cancer line Hs578T (Fig. 4E).

Hsf1 is involved in HIF-1 translation. HIF-1α expression can be regulated at multiple levels, including protein degradation (e.g., following hypoxia or hypoxia mimetics), transcription (e.g., upon exposure to lipopolysaccharide or cytokines), or translation (e.g., upon exposure to autocrine growth factors, like epidermal growth factor or insulin-like growth factor) (see reference 7 for a review). Hsf1 knockdown may block HIF-1α accumulation by affecting any of these mechanisms, and therefore, we addressed what mechanisms are targeted by Hsf1.

To test for transcription and mRNA degradation, we analyzed expression of HIF-1α mRNA by qRT-PCR. For these experi-
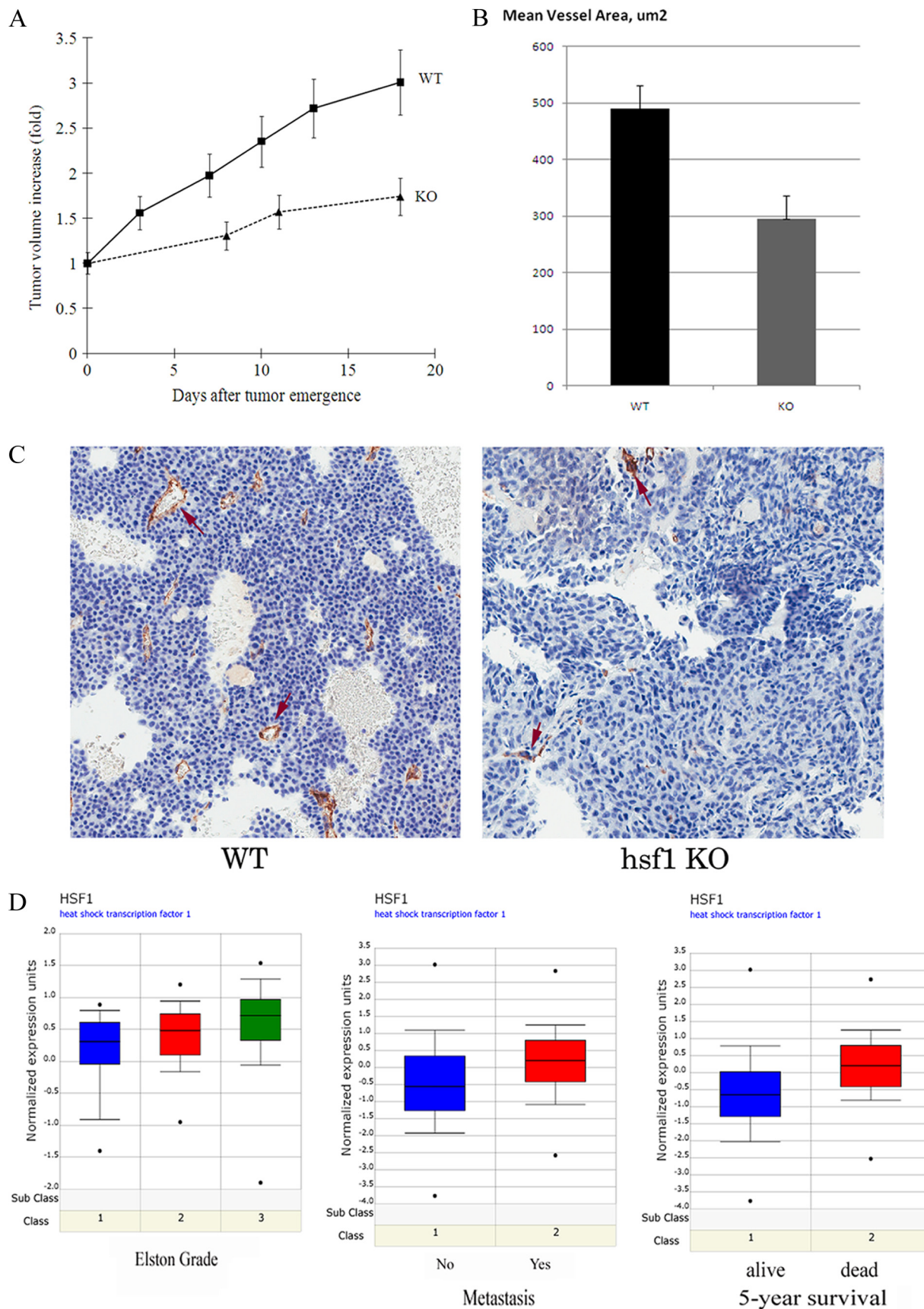
FIG 2 Hsf1 is involved in breast tumor progression. (A) NeuT-induced tumors in *Hsf1* KO mice demonstrate reduced growth rate. The data shown are means ± standard errors of the means. (B) Tumors in *Hsf1*-KO mice demonstrate reduced angiogenesis. Tumors from WT and KO animals were excised, fixed, stained for endothelial marker CD31, and analyzed for mean vessel area. (C) Tumor tissue staining with anti-CD31 antibody. Tumors from control and Hsf1-KO animals are shown. (D) Higher expression of *Hsf1* mRNA in human breast cancer correlates with higher Elston grade, metastasis, and lower 5-year survival according to the Oncomine database (www.oncomine.org).
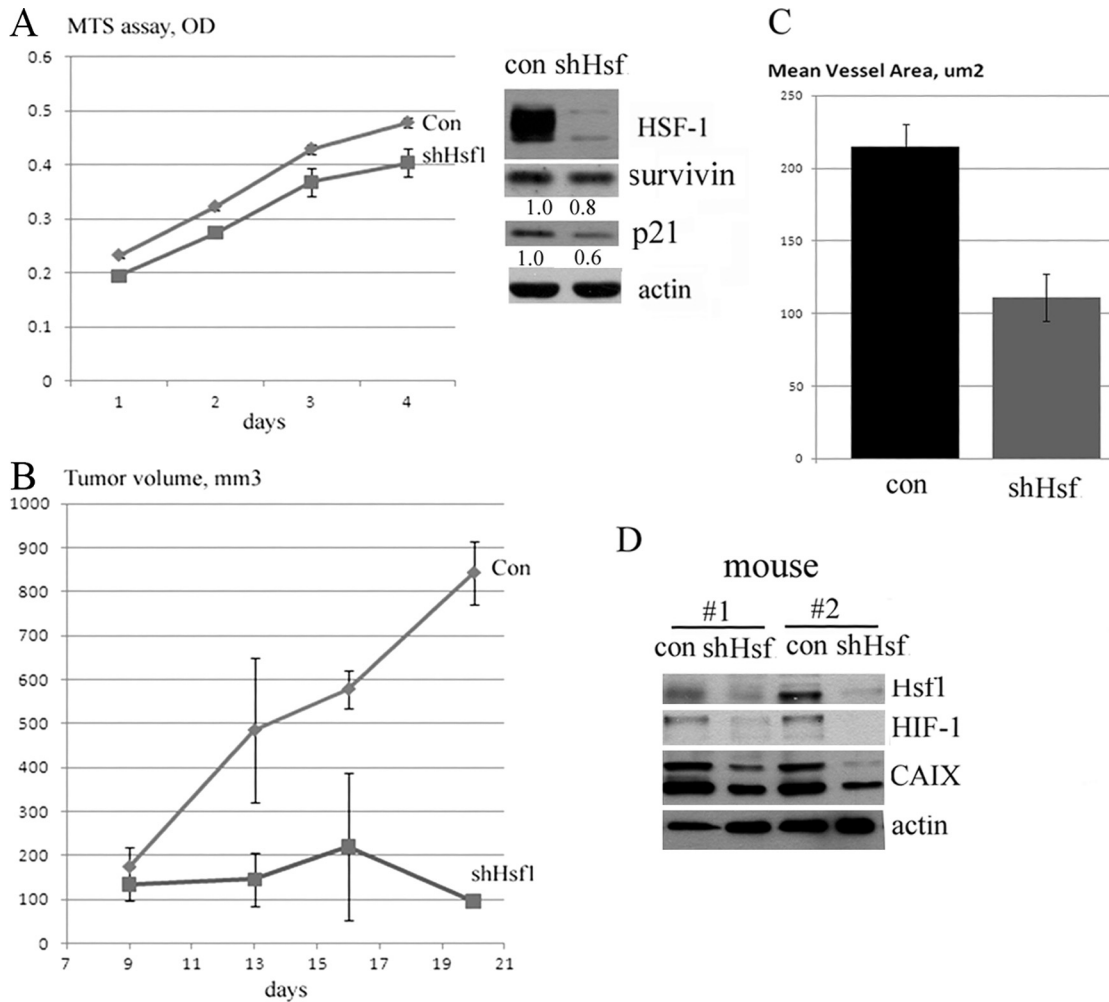
FIG 3 Hsf1 knockdown suppresses growth and angiogenesis of tumors in the xenograft model. (A) Knockdown of Hsf1 has little effect on growth of MCF7 cells *in vitro*, and it does not increase p21 or decrease survivin levels. Cells were infected with shHsf1 retrovirus and selected for 4 days; their growth was assessed by formazan production MTS [3-(4,5-dimethylthiazol-2-yl)-5-(3-carboxymethoxyphenyl)-2-(4-sulfophenyl)-2H-tetrazolium] assay, and expression of p21 and survivin was assessed by immunoblotting. (B) Knockdown of Hsf1 blocks growth of MCF7 cells *in vivo* in xenografts. Cells infected with shHsf1 retrovirus as in panel A were injected in nude mice (10[6] cells per injection), and growth of tumors was monitored by caliper (see Materials and Methods for details). (C) Xenograft tumors from animals (as described in panel B) were excised, fixed, stained for CD31, and analyzed for mean vessel area as in Fig. 2B. Data are means ± standard errors. (D) Knockdown of Hsf1 reduces expression of HIF-1 and its target CAIX in xenografts. Expression of HIF-1 and CAIX tumor xenografts was analyzed by immunoblotting.

ments, we used MCF7 cells which have undetectable levels of HIF-1α under normal conditions but accumulate this protein under hypoxia. We also used Hs578T breast tumor cells, which have elevated basal levels of HIF-1α, but these levels can be further increased by hypoxia mimetics (Fig. 4E and 5B). Although in both lines Hsf1 knockdown markedly reduced expression of HIF-1α protein (Fig. 4A and E and Fig. 5B), there was no downregulation of HIF-1α mRNA levels (Fig. 5A), indicating that Hsf1 regulates HIF-1 by affecting a step in the pathway downstream of HIF-1α mRNA transcription or degradation. To assess stability of HIF-1α protein, we treated cells with a proteasome inhibitor, MG132. If Hsf1 knockdown enhances degradation of HIF-1, inhibition of proteasome should lead to restoration of HIF-1α in Hsf1-depleted cells to levels seen in control cells treated with MG132. In the experiment, MG132 treatment caused robust accumulation of HIF-1α in control cells, but much weaker buildup of HIF-1α was seen in Hsf1-depleted cells (Fig. 4A, C, and D and Fig. 5B). There-

fore, inhibition of protein degradation was insufficient to restore HIF-1 levels, suggesting that the Hsf1-dependent regulation of HIF-1 is at the level not of protein stability but rather of protein synthesis. (Of note, in MG132-treated cells HIF-1 migrated on gels faster than hypoxia-induced HIF-1, apparently due to the absence of phosphorylation [21].) To directly assess the effects of Hsf1 knockdown on HIF-1 degradation, we measured the half-lives of HIF-1 in control and *Hsf1* knockdown MCF7 cells treated with DFO. Samples were taken at different time points following addition of the protein synthesis inhibitor emetine, and HIF-1 levels were analyzed by immunoblotting. In naïve MCF7 cells, degradation of HIF-1α was very fast (half-life [$t_{1/2}$] of about 10 min), while in DFO-treated cells HIF-1α was more stable ($t_{1/2}$ of about 25 min) (Fig. 5C), which is in line with previous reports. While strongly reducing HIF-1α expression levels (Fig. 4A), depletion of Hsf1 did not significantly affect stability of HIF-1 in either control or DFO-
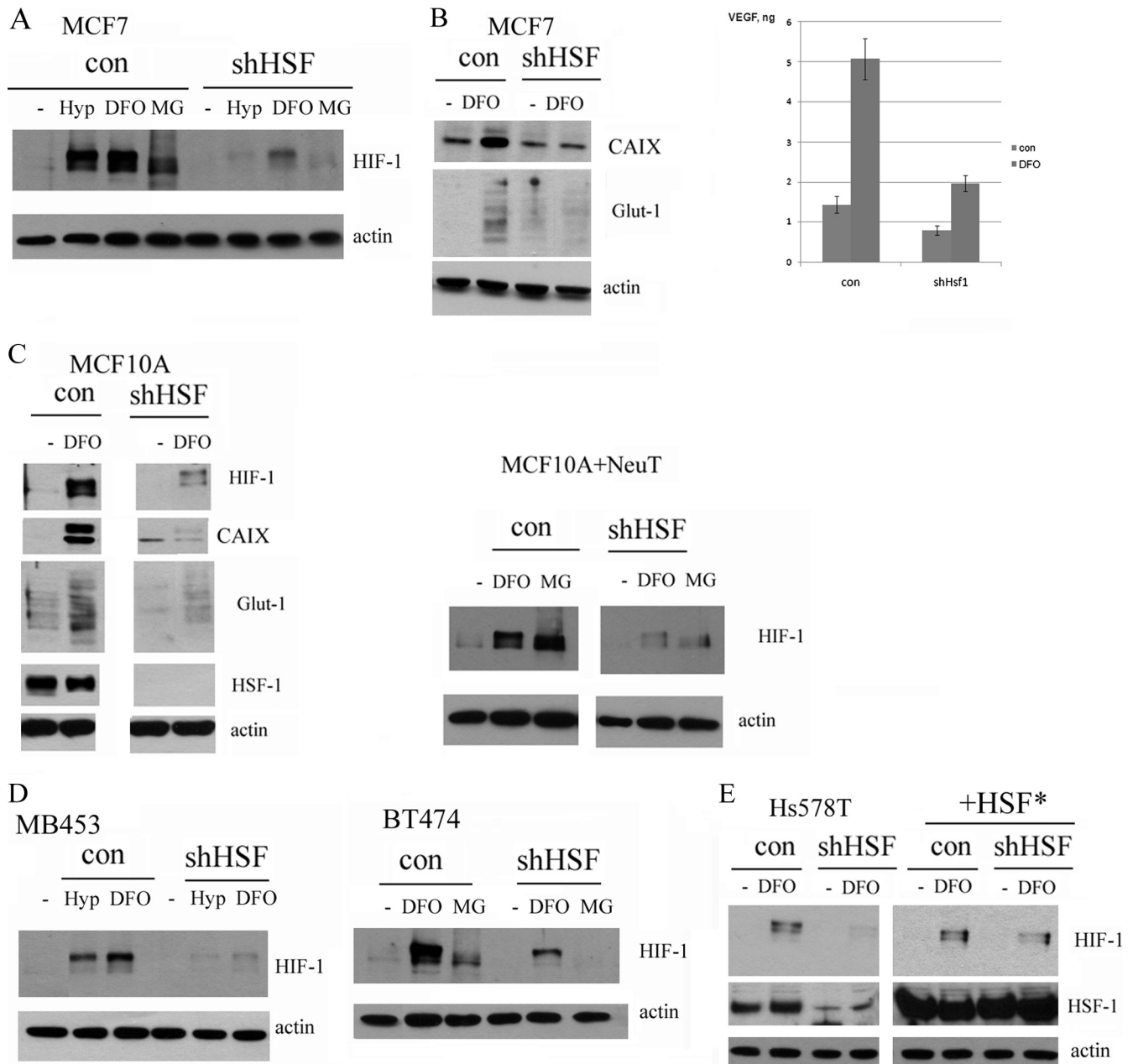
FIG 4 Knockdown of Hsf1 suppresses HIF-1 signaling in cell lines. (A) Knockdown of Hsf1 in MCF7 cells inhibits HIF-1 accumulation after cells were subjected to hypoxia (Hyp, 1% O_2, 16 h) or treated with the hypoxia mimetic DFO (100 μM, 4 h) or proteasome inhibitor MG132 (5 μM, 4 h). Cells were infected with shHsf1 retrovirus as in Fig. 3A, and HIF-1 expression was analyzed by immunoblotting. (B) Hsf1 knockdown reduces induction of HIF-1α targets VEGF, CAIX, and Glut-1 in MCF7 cells. Cells were infected with Hsf1 retrovirus as in panel A and treated with DFO for 48 h, and medium was collected and analyzed by enzyme-linked immunosorbent assay for VEGF by Quansys Biosciences or lysates were blotted with anti-CAIX or anti-Glut-1 antibodies. (C) Knockdown of *Hsf1* inhibits accumulation of HIF-1 and its targets in MCF10A (left panel) and NeuT-infected MCF10A (right panel) cells. Cells were treated with DFO (100 μM, 4 h) or MG132 (5 μM, 4 h), and accumulation of HIF-1 and its targets CAIX and Glut-1 was analyzed by immunoblotting. (D) Her2-positive MB453 (left panel) and BT474 (right panel) cells were infected with Hsf1 retrovirus as in panel A and treated with hypoxia for 16 h or DFO (100 μM, 4 h) or MG132 (5 μM, 4 h), and accumulation of HIF-1 was analyzed by immunoblotting. (E) Expression of the shRNA-resistant Hsf1 mutant reverses the effect of shRNA on HIF-1α. Hs578T cells were infected with retrovirus containing *Hsf1** or control retrovirus and selected. Then Hsf1 was depleted by shRNA, and HIF-1α expression was measured by immunoblotting in naïve cells or following DFO treatments.

treated cells (Fig. 5C). Similarly, *Hsf1* knockdown did not affect the rates of HIF-1α degradation in naïve Hs578T cells, while it decreased HIF-1 levels (Fig. 5C).

To assess translation of HIF-1α directly, cells were pulse-labeled with [^{35}S]methionine for 10 min, and HIF-1α was immu-

noprecipitated with the corresponding antibody. Hsf1 knockdown significantly reduced incorporation of label into HIF-1α (Fig. 5D), which, together with the data that mRNA levels were similar, indicated that the main regulation of HIF-1 by Hsf1 is at the level of translation.
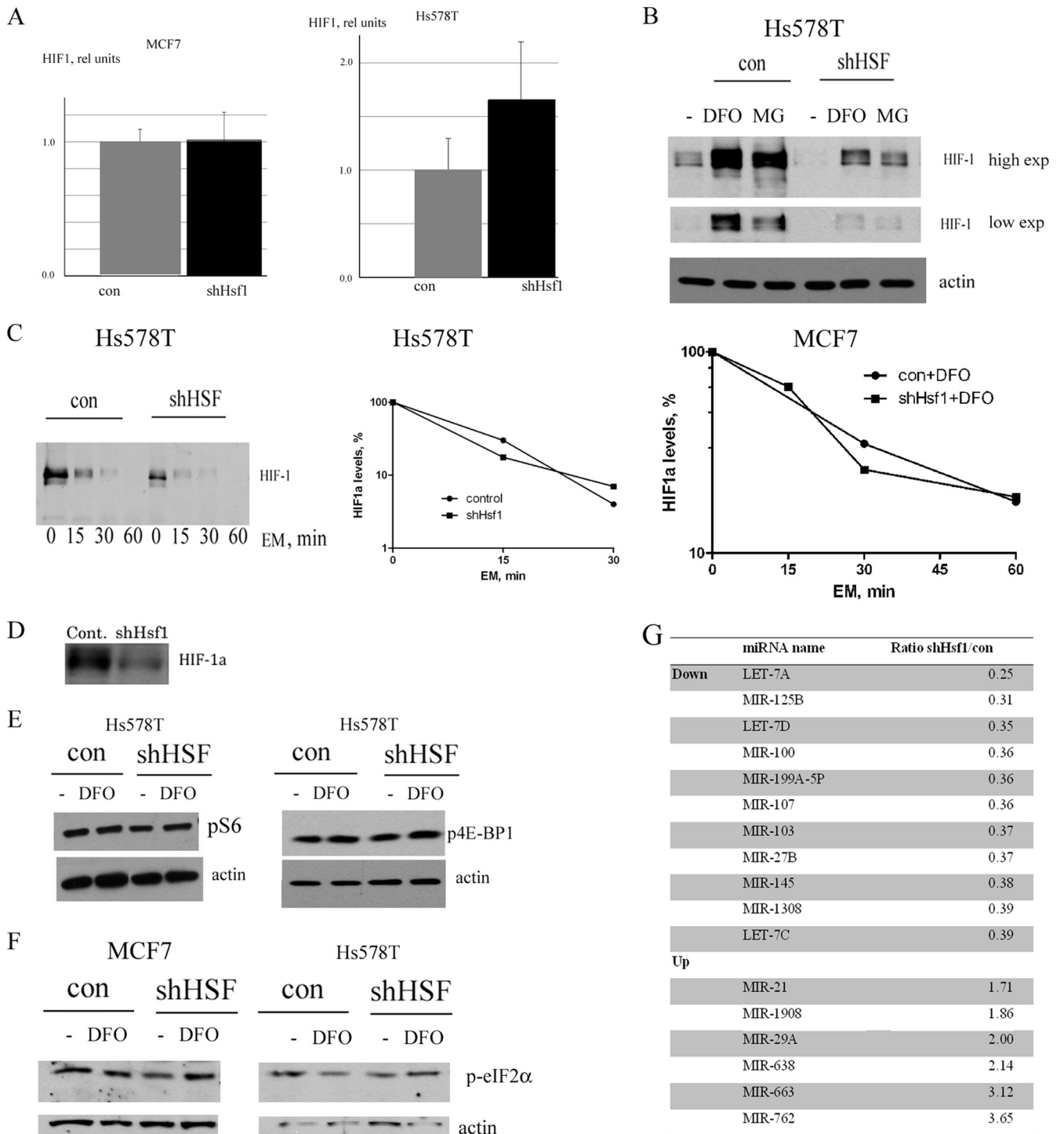
FIG 5 Effect of *Hsf1* knockdown on various levels of HIF-1 expression. (A) Effect of *Hsf1* knockdown on HIF-1α mRNA levels in MCF7 or Hs578T cells; DFO treatment did not change mRNA levels (not shown). qRT-PCR was done as described in Materials and Methods. (B) shHsf1 suppresses both basal and DFO (100 μM, 4 h)- or MG132 (5 μM, 4 h)-induced levels of HIF-1 in Hs578T cells. (C) Knockdown of Hsf1 does not affect stability of HIF-1. Hs578T or MCF7 cells were treated with the protein synthesis inhibitor emetine (EM; 10 μM) in the absence or presence of DFO (100 μM) for the time intervals indicated, and the levels of HIF-1 were determined. The middle panel shows quantification of the left panel. (D) Hsf1 knockdown reduces translation of HIF-1α. MCF7 cells were labeled with [^{35}S]methionine for 10 min, and HIF-1 was immunoprecipitated, run on SDS-PAGE gels, and exposed to film. The initial material was normalized by trichloroacetic acid-precipitable count (label incorporated into proteins). (E) Hsf1 knockdown does not affect activity of mTOR pathway. Activity of the mTOR pathway was assayed by antibody to phosphorylated (Ser235/236) S6 ribosomal protein (left panel) or phosphorylated (Ser65) 4E-BP1 (right panel). (F) Hsf1 knockdown does not affect phosphorylation of eIF2α, assayed by antibody to phosphorylated (Ser51) eIF2α. (G) Effect of shHsf1 knockdown on microRNA profile of Hs578T cells. MicroRNA was isolated and assayed by Miltenyi Biotec. See text for further explanation.

Effects of Hsf1 on major pathways regulating HIF-1α translation and microRNA (miRNA). We further explored effects of Hsf1 on translation of HIF-1α. One possibility involves the mTOR pathway, since HIF-1α translation is dependent on mTOR activity (7, 21, 34). Accordingly, we tested whether Hsf1 knockdown downregulates components of the mTOR pathway, including phospho-S6 ribosomal protein and phospho-4E-BP1, and found no effects of Hsf1 knockdown on either p-S6 or p-4E-BP1 (Fig. 5E). Therefore, the mTOR pathway apparently is not involved in regulation of HIF-1 by Hsf1 depletion.

Another potential mechanism which can regulate HIF-1 translation is associated with downregulation of eIF2α by its phosphorylation on Ser51. We explored this possibility but did not find any difference in eIF2α phosphorylation upon Hsf1 knockdown (Fig. 5F).

Next we used microarrays to assess how Hsf1 knockdown affects levels of microRNAs which may potentially regulate HIF-1α translation. *Hsf1* knockdown had profound effects on expression of a number of microRNAs in Hs578T cells, but none of the upregulated microRNAs had binding sites in the untranslated regions (UTRs) of HIF-1α mRNA. Therefore, these miRNAs cannot be directly involved in regulation of HIF-1α (Fig. 5G). On the other hand, interestingly, 7 out of 11 microRNAs reduced upon Hsf1 knockdown (i.e., Let-7A, Let-7C, Let-7D, MiR-199A-5P, MiR-210, MiR-125B, and MiR-107) were previously shown to be upregulated by HIF-1 or hypoxia (23) (Fig. 5F). Therefore, downregulation of these microRNAs upon *Hsf1* knockdown most likely reflects suppression of HIF-1. Importantly, some of these miRNAs, e.g., Let-7 and MiR-125, regulate multiple targets involved in cancer, e.g., RAS, MYC, and p53 (12). Accordingly, effects of Hsf1 on HIF-1 not only result in suppression of angiogenesis but stimulate a variety of cancer-related pathways.

Hsf1 knockdown downregulates HuR and its targets associated with cancer traits. Among regulators of HIF-1α translation, there are mRNA-binding proteins PTBP1 and HuR. Since the mTOR pathway, eIF2α, or microRNA was not involved in HIF-1 regulation by *Hsf1*, we assessed expression of PTBP1 and HuR upon Hsf1 knockdown. By immunoblotting, we did not find any decrease in PTBP1 levels (Fig. 6A). On the other hand, HuR levels decreased by about 70% upon *Hsf1* knockdown in both MCF7 and Hs578 cells (Fig. 6A). Furthermore, we found 70 to 80% downregulation of HuR levels in MCF7 xenografts as well (Fig. 6B), suggesting that this factor may be involved in HIF-1 regulation by Hsf1. With many targets, HuR regulates stability of mRNA; however, specifically with HIF-1, it was demonstrated that HuR regulates its translation without affecting mRNA stability (17). Therefore, effects of HuR on HIF-1 are consistent with our results with qRT-PCR (Fig. 5A).

To test whether downregulation of HuR is responsible for suppression of HIF-1 upon *Hsf1* knockdown, we first assessed whether decrease in HuR levels by shRNA can downregulate HIF-1 in cell lines which we used for the study. Indeed, as seen in Fig. 6C, downregulation of HuR markedly suppressed HIF-1 accumulation in both MCF7 and Hs578T cells. Furthermore, we assessed whether overexpression of HuR can prevent effect of *Hsf1* knockdown on HIF-1 accumulation. Hs578T and MCF7 cells were first infected with retrovirus expressing HuR, selected with neomycin, and then infected with shHsf1 retrovirus and selected with puromycin. HuR overexpression completely prevented an effect of Hsf1 knockdown on HIF-1 accumulation in both Hs578T

and MCF7 cells (Fig. 6D). These results demonstrate that downregulation of HuR by Hsf1 knockdown appears to be the major mechanism responsible for HIF-1 inhibition.

We next addressed whether *Hsf1* affects *HuR* transcription, translation, or degradation. Hsf1 apparently did not affect HuR protein stability, since addition of the proteasome inhibitor MG132 did not restore HuR levels in shHsf1 cells (data not shown). At the same time, shHsf1 decreased levels of HuR mRNA (Fig. 6E). This effect was apparently at the level of transcription, since we did not observe any effect on the *HuR* mRNA stability (Fig. 6F). Furthermore, we measured levels of *HuR* mRNA and protein in *Hsf1*-KO animals. In line with results of the cell culture experiments, *Hsf1*-KO mice had significantly lower levels of HuR than did control mice (Fig. 6G). These data emphasize the relevance of the role of Hsf1 in regulation of HuR to the mammalian organism.

Along with overexpression of Hsf1 and HIF-1, tumor progression in various human cancers is associated with higher expression of HuR (24, 25). HuR controls mRNA stability and/or translation of many proteins involved in cancer, including proteins involved in angiogenesis (e.g., HIF-1, HIF-2, and vascular endothelial growth factor [VEGF]), cell survival (e.g., p53 and Sirt1), proliferation (e.g., cyclins, Cdc2, and p21), and others (1, 14, 24, 25). Since *Hsf1* knockdown leads to HuR decrease, we assessed whether some of the known targets of HuR are also downregulated in these cells. Indeed, along with HIF-1 and VEGFA, knockdown of Hsf1 in Hs578 or MCF7 cells decreased levels of other known targets of HuR such as HIF-2, Sirt1, p53, and cyclin B (Fig. 6H to J). Therefore, by regulating HuR, Hsf1 controls a multitude of genes and pathways involved in various stages of tumorigenesis, including initiation, invasion, and angiogenesis.

DISCUSSION

Previous studies demonstrated that human cancers often have higher levels of expression of Hsf1 and heat shock proteins, which are associated with tumor progression and resistance to anticancer therapy, thus indicating that Hsf1 and Hsps play an important role in cancer. Indeed, recent works using knockout mice demonstrated that Hsf1 is essential for tumorigenesis induced by RAS or *p53* knock-in mutant (R172H). Following these developments, we attempted to dissect the mechanism of Hsf1 effects on tumorigenesis and found that Hsf1 interferes with senescence signaling, thus playing a critical role in prevention of oncogene-induced senescence (OIS). We demonstrated that when Hsf1 or Hsp72 is downregulated, the Her2/NeuT oncogene can no longer transform mammary epithelial cells but instead causes senescence which is accompanied by accumulation of a cell cycle inhibitor, p21, and decrease in levels of the cell cycle promoter and apoptosis inhibitor survivin (28, 29). Furthermore, in established Her2-positive human breast cancer lines, knockdown of Hsf1 led to an increase in p21, a decrease in survivin, and inhibition of their growth (28). Due to this mechanism, Hsf1 is essential for transformation of human mammary epithelial cells by the Her2/NeuT oncogene and maintenance of growth.

These findings suggested that Hsf1 should mainly function at early stages of cancer development when the Her2 oncogene is activated and OIS blocks cell proliferation and transformation. Indeed, here we demonstrate that in Hsf1-KO mice emergence of tumors driven by the Her2/NeuT oncogene is dramatically suppressed. There was no NeuT-induced hyperplasia of mammary
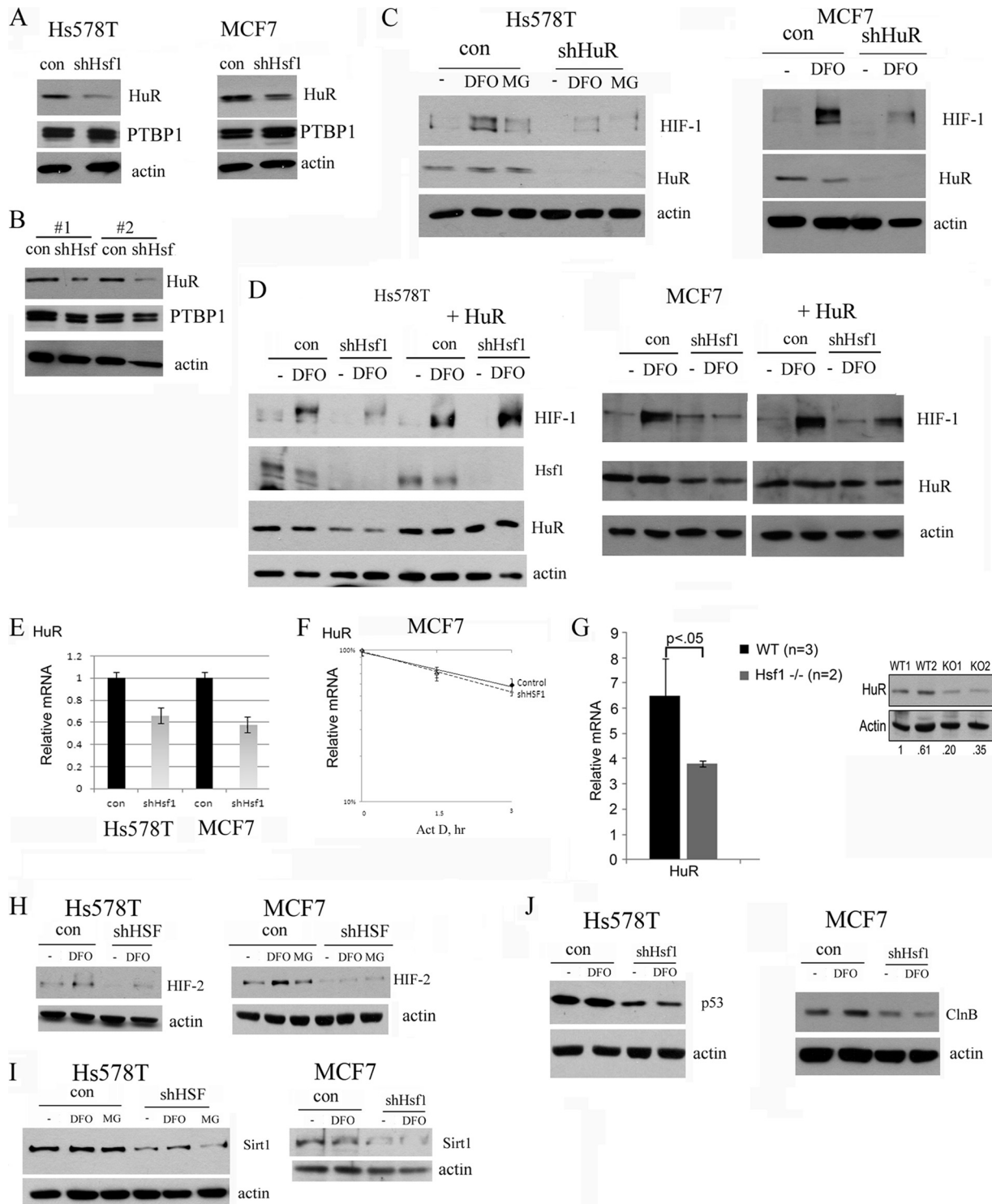
FIG 6 Suppression of HIF-1 accumulation by shHsf1 is associated with HuR downregulation. (A) *Hsf1* knockdown decreases HuR but not PTBP1 levels in Hs578T (left panel) and MCF7 (right panel) cells. (B) *Hsf1* knockdown decreases HuR but not PTBP1 levels in MCF7 xenografts (Fig. 3B to D). (C) Knockdown of *HuR* suppresses HIF-1 accumulation in Hs578T (left panel) and MCF7 (right panel) cells. Cells were infected with shHuR retrovirus, selected, and treated with DFO (100 μM) or MG132 (5 μM) for 4 h. (D) HuR overexpression prevents inhibition of HIF-1 accumulation by Hsf1 knockdown. Hs578T and MCF7 cells were first infected with HuR retrovirus and selected. HuR-expressing cells were infected with shHsf1 retrovirus as described in Materials and Methods and treated with 100 μM DFO for 4 h. (E) Hsf1 knockdown leads to reduction of HuR mRNA levels in Hs579T and MCF7 cells. (F) *Hsf1* knockdown does not affect stability of *HuR* mRNA. Levels of HuR mRNA were measured by qRT-PCR after inhibition of transcription by actinomycin at the indicated time points. (G) Levels of *HuR* mRNA and protein were assessed in liver of control and Hsf1-KO mice. (H to J) Hs578T and MCF7 cells were infected with shHsf1 retrovirus as in Fig. 4A and 5B and treated with DFO (100 μM) or MG132 (5 μM) for 4 h, and the levels of HIF-2α (H), Sirt1 (I), p53 (mutant) (J), or cyclin B (ClnB) (J) were assayed by immunoblotting.

tissue and development of alveoli was strongly reduced (Fig. 1), further supporting the notion that Hsf1 is essential early in tumor development.

These effects of *Hsf1* KO were almost indistinguishable from effects of *Hsp72* KO, which, as we recently demonstrated, also inhibits mammary tissue hyperplasia and alveolar development, causes senescence of epithelial cells, and overall blocks tumor initiation (29). These data are consistent with our prior suggestion that the major effect of Hsf1 depletion on OIS may be mediated by downregulation of Hsp72. Indeed, we found that in cell lines where depletion of Hsf1 causes downregulation of Hsp72, it also causes OIS, while in cell lines where depletion of Hsf1 does not cause Hsp72 downregulation, it does not trigger OIS (unpublished data). Nevertheless, the mechanism of OIS remains in these latter lines, since depletion of Hsp72 in them does trigger OIS (16).

Effects of Hsf1 on cancer are not limited to the control of OIS, and literature data suggest that Hsf1 plays a more general role in tumor development. For example, it was demonstrated that in a series of prostate cancer clones that developed invasiveness and metastasis upon passage through nude mice, expression of Hsf1 was further increased in more aggressive tumorigenic clones (2). Furthermore, data from the cancer microarray archive Oncomine also indicate that levels of Hsf1 correlate with the tumor grade, ultimately indicating that besides tumor initiation Hsf1 should be involved in tumor progression (Fig. 2C).

Based on these considerations, we addressed the role of Hsf1 in tumor progression, focusing on a mouse model of Her2-positive breast cancer. Initially, we looked at rare tumors that emerged in *Hsf1*-KO animals that express NeuT. Of note, these tumors emerged much later than did tumors in control NeuT-expressing mice (Fig. 1B). Importantly, tumors in Hsf1-knockout mice grew much slower than in control mice (Fig. 2A), further confirming that in addition to tumor initiation, Hsf1 plays a role in tumor growth.

In these rare tumors emerging in *Hsf1*-KO animals, we observed that angiogenesis is impaired, which may be a factor in slow growth. In order to investigate mechanisms of these effects, we had to develop xenograft and cell culture models. Testing several breast cancer mammary epithelium lines in culture demonstrated that levels of the major regulator of angiogenesis HIF-1 are dramatically reduced upon depletion of Hsf1. The xenograft model was more difficult to apply, since cancer cell lines usually develop senescence or apoptosis following Hsf1 depletion (13, 28), and lack of growth in xenografts could be due to OIS or apoptosis, rather than insufficient angiogenesis. After screening of a collection of breast cancer lines, we found that in two lines, MCF7 and Hs578T, depletion of Hsf1 does not downregulate Hsp72 and does not cause senescence, while it does cause downregulation of HIF-1α. Accordingly, MCF7 cells with depleted Hsf1 could form tumors in xenografts, but after emergence tumors grew very slowly and had reduced angiogenesis. This model therefore recapitulates suppression of tumor progression seen in the knockout animals. An interesting conclusion from these experiments is that while Hsf1 effects on OIS and tumor initiation are mediated by Hsp72, effects on HIF-1 and tumor progression are independent of Hsp72 and must involve distinct Hsf1 transcription targets.

Interestingly, there are very complex bidirectional relations between heat shock transcription factors and HIF-1. For example, it has been demonstrated in *Drosophila* that hypoxia induces heat shock response via HIF-1 (3). On the other hand, in mammalian cells Hsf2 and Hsf4 were shown to regulate HIF-1 transcription (10).

In addition to angiogenesis, HIF-1 regulates expression of genes involved in other aspects of tumorigenesis, including survival of hypoxia and other harmful conditions, invasion, etc. We have found that beyond angiogenesis-related targets of HIF-1 (e.g., VEGF), Hsf1 also controls expression of Glut-1 and CAIX and most likely other HIF-regulated genes involved in tumor progression. For example, Hsf1 regulates a set of cancer-related miRNAs (e.g., Let-7, MiR-199A, or MiR-125B), which are known to be controlled by HIF-1 or hypoxia (23).

In the search for a molecular mechanism of the effect of Hsf1 on HIF-1, we found that Hsf1 controls another major regulator of tumor progression, HuR. HIF-1 accumulation under hypoxia is mediated by inhibition of constitutive ubiquitination by the E3 ligase VHL, resulting in suppression of HIF-1α degradation by the proteasome. Originally, we suggested that Hsf1 deficiency increases the rate of HIF-1α degradation. However, direct measurement of the rate of HIF-1α degradation showed that Hsf1 knockdown does not increase the half-life of HIF-1α. Similarly, we found that there is no difference in the levels of HIF-1α mRNA in Hsf1-depleted cells. Therefore, *Hsf1* knockdown does not affect either degradation of HIF-1α protein or transcription of degradation of HIF-1α mRNA, and indeed we found that Hsf1 regulates HIF-1α translation (Fig. 5). Assessing major mechanisms known to regulate HIF-1 translation (miRNAs, mTOR, and eIF2α pathways), we could not implicate any of these mechanisms in regulation of HIF-1 translation following Hsf1 knockdown. On the other hand, there was a marked decrease in the levels of the mRNA-binding protein HuR, a major regulator of translation which is known to promote translation of HIF-1α (Fig. 6). This decrease was seen both in cell culture and in xenograft tumors as well in Hsf1-knockout animals (Fig. 6). Effects of Hsf1 on HIF-1 were mediated by HuR, since knockdown of HuR suppressed HIF-1 accumulation in our models, while restoration of HuR levels in Hsf1-depleted cells prevented HIF-1 downregulation (Fig. 6). These data demonstrate that downregulation of HuR is the main mechanism by which Hsf1 regulates HIF-1 translation.

HuR is overexpressed in various human cancers, and its expression correlates with cancer progression (1, 14, 24, 25). Besides HIF-1, HuR controls mRNA stability and translation of a plethora of proteins associated with cancer, and we report that several known cancer-related targets of HuR, including HIF-2, Sirt1, p53, and cyclin B, are also downregulated upon Hsf1 knockdown (Fig. 6). Therefore, we have established an important link between Hsf1 and two major players in cancer progression, HIF-1 and HuR. This association between Hsf1, HuR, and HIF-1 demonstrates that Hsf1 is essential not only for initial stages of tumorigenesis by preventing oncogene-induced senescence but also for progression of established tumors.

ACKNOWLEDGMENT

REFERENCES

1. **Abdelmohsen K, Lal A, Kim HH, Gorospe M.** 2007. Posttranscriptional orchestration of an anti-apoptotic program by HuR. Cell Cycle **6**:1288–1292.

2. **Akalin A, et al.** 2001. A novel mechanism for chaperone-mediated telomerase regulation during prostate cancer progression. Cancer Res. **61:** 4791–4796.

3. **Baird NA, Turnbull DW, Johnson EA.** 2006. Induction of the heat shock pathway during hypoxia requires regulation of heat shock factor by hypoxia-inducible factor-1. J. Biol. Chem. **281:**38675–38681.

4. **Beere HM.** 2005. Death versus survival: functional interaction between the apoptotic and stress-inducible heat shock protein pathways. J. Clin. Invest. **115:**2633–2639.

5. **Ben-Porath I, Weinberg RA.** 2005. The signals and pathways activating cellular senescence. Int. J. Biochem. Cell Biol. **37:**961–976.

6. **Bihani T, et al.** 2004. Differential oncogenic Ras signaling and senescence in tumor cells. Cell Cycle **3:**1201–1207.

7. **Brahimi-Horn MC, Pouyssegur J.** 2009. HIF at a glance. J. Cell Sci. **122:**1055–1057.

8. **Braig M, Schmitt CA.** 2006. Oncogene-induced senescence: putting the brakes on tumor development. Cancer Res. **66:**2881–2884.

9. **Chang B-D, et al.** 2002. Molecular determinants of terminal growth arrest induced in tumor cells by a chemotherapeutic agent. Proc. Natl. Acad. Sci. U. S. A. **99:**389–394.

10. **Chen R, Liliental JE, Kowalski PE, Lu Q, Cohen SN.** 2011. Regulation of transcription of hypoxia-inducible factor-1alpha (HIF-1alpha) by heat shock factors HSF2 and HSF4. Oncogene **30:**2570–2580.

11. **Ciocca DR, Calderwood SK.** 2005. Heat shock proteins in cancer: diagnostic, prognostic, predictive, and treatment implications. Cell Stress Chaperones **10:**86–103.

12. **Croce CM.** 2009. Causes and consequences of microRNA dysregulation in cancer. Nat. Rev. Genet. **10:**704–714.

13. **Dai C, Whitesell L, Rogers AB, Lindquist S.** 2007. Heat shock factor 1 is a powerful multifaceted modifier of carcinogenesis. Cell **130:**1005–1018.

14. **Danilin S, et al.** 2010. Role of the RNA-binding protein HuR in human renal cell carcinoma. Carcinogenesis **31:**1018–1026.

15. **Gabai VL, Mabuchi K, Mosser DD, Sherman MY.** 2002. Hsp72 and stress kinase c-jun N-terminal kinase regulate the Bid-dependent pathway in tumor necrosis factor-induced apoptosis. Mol. Cell. Biol. **22:**3415–3424.

16. **Gabai VL, Yaglom JA, Waldman T, Sherman MY.** 2009. Heat shock protein Hsp72 controls oncogene-induced senescence pathways in cancer cells. Mol. Cell. Biol. **29:**559–569.

17. **Galban S, et al.** 2008. RNA-binding proteins HuR and PTB promote the translation of hypoxia-inducible factor 1alpha. Mol. Cell. Biol. **28:**93–107.

18. **Gordan JD, Simon MC.** 2007. Hypoxia-inducible factors: central regulators of the tumor phenotype. Curr. Opin. Genet. Dev. **17:**71–77.

19. **Guy CT, et al.** 1992. Expression of the neu protooncogene in the mammary epithelium of transgenic mice induces metastatic disease. Proc. Natl. Acad. Sci. U. S. A. **89:**10578–10582.

20. **Hunt CR, et al.** 2004. Genomic instability and enhanced radiosensitivity in Hsp70.1- and Hsp70.3-deficient mice. Mol. Cell. Biol. **24:**899–911.

21. **Ke Q, Costa M.** 2006. Hypoxia-inducible factor-1 (HIF-1). Mol. Pharmacol. **70:**1469–1480.

22. **Khaleque M, et al.** 2005. Induction of heat shock proteins by heregulin beta1 leads to protection from apoptosis and anchorage-independent growth. Oncogene **24:**6564–6573.

23. **Kulshreshtha R, Davuluri RV, Calin GA, Ivan M.** 2008. A microRNA component of the hypoxic response. Cell Death Differ. **15:**667–671.

24. **Lopez de Silanes I, et al.** 2003. Role of the RNA-binding protein HuR in colon carcinogenesis. Oncogene **22:**7146–7154.

25. **Lopez de Silanes I, Lal A, Gorospe M.** 2005. HuR: post-transcriptional paths to malignancy. RNA Biol. **2:**11–13.

26. **Lowe SW, Cepero E, Evan G.** 2004. Intrinsic tumour suppression. Nature **432:**307–315.

27. **McMillan DR, Xiao X, Shao L, Graves K, Benjamin IJ.** 1998. Targeted disruption of heat shock transcription factor 1 abolishes thermotolerance and protection against heat-inducible apoptosis. J. Biol. Chem. **273:**7523–7528.

28. **Meng L, Gabai VL, Sherman MY.** 2010. Heat-shock transcription factor HSF1 has a critical role in human epidermal growth factor receptor-2-induced cellular transformation and tumorigenesis. Oncogene **29:**5204–5213.

29. **Meng L, Hunt C, Yaglom JA, Gabai VL, Sherman MY.** 2011. Heat shock protein Hsp72 plays an essential role in Her2-induced mammary tumorigenesis. Oncogene **30:**2836–2845.

30. **Min J-N, Huang L, Zimonjic DB, Moskophidis D, Mivechi NF.** 2007. Selective suppression of lymphomas by functional loss of Hsf1 in a p53-deficient mouse model for spontaneous tumors. Oncogene **26:**5086–5097.

31. **Muller WJ, et al.** 1996. Synergistic interaction of the Neu proto-oncogene product and transforming growth factor alpha in the mammary epithelium of transgenic mice. Mol. Cell. Biol. **16:**5726–5736.

32. **Page TJ, et al.** 2006. Genome-wide analysis of human HSF1 signaling reveals a transcriptional program linked to cellular adaptation and survival. Mol. Biosyst. **2:**627–639.

33. **Pirkkala L, Nykanen P, Sistonen L.** 2001. Roles of the heat shock transcription factors in regulation of the heat shock response and beyond. FASEB J. **15:**1118–1131.

34. **Semenza GL.** 2010. Defining the role of hypoxia-inducible factor 1 in cancer biology and therapeutics. Oncogene **29:**625–634.

35. **Solimini NL, Luo J, Elledge SJ.** 2007. Non-oncogene addiction and the stress phenotype of cancer cells. Cell **130:**986–988.

36. **Xiao X, et al.** 1999. HSF1 is required for extra-embryonic development, postnatal growth and protection during inflammatory responses in mice. EMBO J. **18:**5943–5952.

37. **Zaarur NG, Porco VLJ, Calderwood S, Sherman M.** 2006. Targeting heat shock response to sensitize cancer cell to proteasome and Hsp90 inhibitors. Cancer Res. **66:**1783–1791.

The heat shock transcription factor Hsf1 is downregulated in DNA damage–associated senescence, contributing to the maintenance of senescence phenotype

Geunwon Kim,[1,2] Anatoli B. Meriin,[2] Vladimir L. Gabai,[2] Elisabeth Christians,[3] Ivor Benjamin,[4] Andrew Wilson,[1] Benjamin Wolozin[5] and Michael Y. Sherman[2]

[1]Department of Medicine, Boston University School of Medicine, Boston, MA 02118, USA
[2]Department of Biochemistry, Boston University School of Medicine, Boston, MA 02118, USA
[3]Université Toulouse III, Centre de Biologie du Développement (UPS-UMR5547), Toulouse Cedex 09, France
[4]Department of Internal Medicine, University of Utah School of Medicine, Salt Lake City, UT 84132, USA
[5]Department of Pharmacology, Boston University School of Medicine, Boston, MA 02118, USA

Summary

Heat shock response (HSR) that protects cells from proteotoxic stresses is downregulated in aging, as well as upon replicative senescence of cells in culture. Here we demonstrate that HSR is suppressed in fibroblasts from the patients with segmental proge-rioid Werner Syndrome, which undergo premature senescence. Similar suppression of HSR was seen in normal fibroblasts, which underwent senescence in response to DNA damaging treatments. The major DNA-damage-induced signaling (DDS) pathways p53–p21 and p38-NF-kB-SASP contributed to the HSR suppression. The HSR suppression was associated with inhibition of both activity and transcription of the heat shock transcription factor Hsf1. This inhibition in large part resulted from the downregulation of SIRT1, which in turn was because of decrease in the expression of the translation regulator HuR. Importantly, we uncovered a posi-tive feedback regulation, where suppression of Hsf1 further acti-vates the p38–NF-κB-SASP pathway, which in turn promotes senescence. Overexpression of Hsf1 inhibited the p38–NFκB-SASP pathway and partially relieved senescence. Therefore, downregu-lation of Hsf1 plays an important role in the development or in the maintenance of DNA damage signaling-induced cell senescence.
Key words: heat shock response; Hsp70; HuR; inflammation; p38; p53; SIRT1.

Introduction

Aging is the most important risk factor in the development of neurode-generative and cardiovascular diseases, diabetes, osteoporosis, and many types of cancer. Various age-associated disorders are characterized by accumulation of damaged proteins (Jana *et al.*, 2000; Koyama *et al.*, 2006; Rahman *et al.*, 2010; Sakellariou *et al.*, 2011). Accordingly, the

Correspondence
Michael Y. Sherman, Department of Biochemistry, K-323, Boston University School of Medicine, Boston, MA 02118, USA. Tel.: +1 617 638 5971; fax: +1 617 638 5339; e-mail: sherma1@bu.edu

reduced capacity to handle misfolded protein has been implicated in the etiology of the disease process (Sherman & Goldberg, 2001). Protein aggregation and accumulation of damaged species in aging reflect the collapse in protein homeostasis (proteostasis; Ben-Zvi *et al.*, 2009; Taylor & Dillin, 2011), which in part results from the reduced ability to induce heat shock proteins that function as molecular chaperones in protein folding and degradation (Wu *et al.*, 1993; Heydari *et al.*, 1994). In turn, malfunction of the heat shock response (HSR) can shorten lifespan of the organism (Hsu *et al.*, 2003). In fact, in *Caenorhabditis elegans* model, suppression of HSR by downregulation of the heat shock transcription factor Hsf1 shortens the lifespan, while overexpression of Hsf1 extends it (Morley & Morimoto, 2004; Ben-Zvi *et al.*, 2009). As Hsf1 has been impli-cated both in aging and in disease, understanding its regulation as well as the effects of Hsf1 on aging and disease is of primary importance.

A NAD+-dependent deacetylase SIRT1 has been implicated in control of Hsf1. SIRT1 was found to deacetylate Hsf1 and keep it associated with the promoter region of heat shock proteins, thus enhancing the overall transcription from the Hsf1-responsive promoters (Westerheide *et al.*, 2009). In line with this finding, caloric restriction, which delays aging by increasing SIRT1 activity, increased HSR in aging rats (Heydari *et al.*, 1993). This finding provides a link between the organism aging and downregulation of HSR.

Certain features of the aging paradigm can be recapitulated in cell cul-ture, where cells undergo replicative senescence. For example, downre-gulation of HSR was demonstrated in fibroblasts that underwent senescence following multiple passages in culture (Lee *et al.*, 1996). Inter-estingly, SIRT1 levels decrease in replicatively senescent cells (Sasaki *et al.*, 2006), suggesting that this factor may be involved in downregulation of HSR in senescence. Among various factors that regulate SIRT1, HuR binds to SIRT1 mRNA and increases its stability, and ultimately its translation (Fan & Steitz, 1998; Abdelmohsen *et al.*, 2007). Levels of HuR also dimin-ish in senescent cells, suggesting that HuR may mediate the effects of senescence on SIRT1, and consequently on Hsf1.

Cell senescence results from the activation of DNA damage signaling (DDS) (Vaziri *et al.*, 1997; Robles & Adami, 1998; Chang *et al.*, 1999). Among DDS pathways, the p53–p21 pathways trigger the senescence, while the so-called senescence-associated secretion phenotype (SASP) is responsible for senescence maintenance (Rodier *et al.*, 2009; Freund *et al.*, 2011). SASP represents secretion of a variety of signaling mole-cules, for example, IL-6, IL-1 or IL-8, controlled by the activation of p38MAPK and NF-κB (Acosta *et al.*, 2008; Orjalo *et al.*, 2009). In addi-tion, p38MAPK regulates a distinct senescence factor p16 (Du *et al.*, 2009).

As a model of aging, we chose fibroblasts from patients with Werner Syndrome (WS). WS is caused by a mutation in the *WRN* gene that pre-sents with premature aging (Goto, 1997). Fibroblasts from patients with WS demonstrate premature senescence and show accumulation of DNA damage (Wyllie *et al.*, 2000).

Here, we investigated the role of DNA damage in the suppression of HSR. Specifically, we probed the main DDS pathways as potential modu-lators of HSR. We found that Hsf1 activity decreases in DDS-induced senescence in part because of the changes in SIRT1 and HuR. Further-

more, we found a new role of Hsf1 as a modulator of senescence pheno-type (Experimental procedures are given in Supporting information).

Results

DNA-damage-induced senescence is associated with suppression of the HSR

To understand how HSR is modulated in aging, we investigated HSR in skin fibroblasts isolated from prematurely aging patients with WS. We used fibroblasts isolated from three patients with WS aged between 19 and 30 at passages 4 to 11 and fibroblasts from normal individuals as age-matched controls, ages between 22 and 27 at passage 14 to 16. Previously, WS fibroblasts were found to undergo premature senescence (Goto, 1997). We observed the typical senescent morphology, including enlargement, flattening, and vacuolization, in WS fibroblasts, which was of a stark contrast to fibroblasts from an age-matched subject (Fig. S1). To assess the HSR in WS, cells were incubated at 43 °C for 35 min, left to recover for 6 h, and expression of the major inducible heat shock protein Hsp70 was measured by immunoblotting. These conditions for HSR were used throughout the study. Compared to fibroblasts from age-matched healthy subjects, WS fibroblasts demonstrated strong decrease in the induction of Hsp70 (Fig. 1A). Unlike finite lifespan WS fibroblasts, hTERT-immortalized WS cells did not show suppressed HSR compared with normal hTERT-immortalized fibroblasts (Fig. S2).Therefore, we suggested that downregulation of the HSR in WS fibroblasts could be associated with premature senescence.

The premature aging phenotype of WS, which is caused by the mutation in the DNA helicase *WRN* gene, is associated with DNA instability (Rossi *et al.*, 2010). Diminished induction of Hsp70 in WS fibroblasts could be connected to the DNA damage. Accordingly, we tested whether DNA damaging treatments in normal cells could have a similar suppressive effect on the HSR. Normal human diploid fibroblasts TIG-1 in early passage (between p12 and p15) were treated with 100 nm doxorubicin (Dox) overnight or exposed to 10 Gy γ–irradiation (IR) and then cultured for 5 days. By day 4, such treatments led to withdrawal from the cell cycle, as indicated by reduced Ki-67 staining, and increased senescence-associated β-galactosidase activity (SA-β-gal). These features corresponded to the appearance of senescence phenotype, well in agreement with previous reports (Chang *et al.*, 1999; Fig. S2A,B). As observed with WS fibroblasts, normal fibroblasts exposed to DNA damaging agents showed significantly suppressed induction of Hsp70 (Fig. 1B). Therefore, similar to replicative senescence, premature senescence by DNA damage causes suppression of the HSR in both normal and disease, and establishes a useful model to investigate the relationship between senescence and the HSR (Fig. 6I).

DNA-damage-induced signaling (DDS) pathways regulate HSR

DNA damage can activate the p53 and the p38MAPK signaling pathways, both of which contribute to the development of senescence (Rodier *et al.*, 2009; Freund *et al.*, 2011). Here, we tested the contribution of each pathway in the suppression of HSR. By day 5 post-treatment, γ-irra-
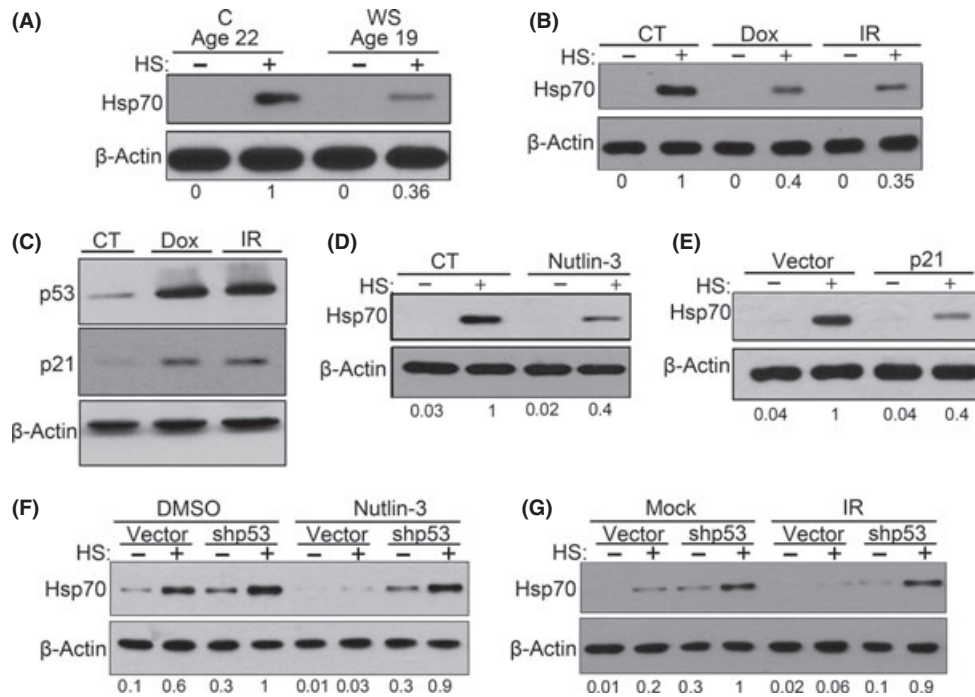
Fig. 1. Activation of p53 pathway caused suppression of HSR. (A) WS fibroblasts (passage 4) and age-matched C fibroblasts (passage 15) were heat shocked and were collected for immunoblotting. (B) TIG-1 fibroblasts were treated with 100 nm of Dox overnight or 10 Gy IR. After 6 days, cells were heat shocked and incubated for 6 h before collection. (C) Same cells from (B) were immunoblotted for indicated proteins. (D) Cells that were induced senescent by 5 days of 10 μm nutlin-3 treatment were heat shocked, and Hsp70 levels were measured. (E) Hsp70 accumulation after heat shock in cells that overexpress p21. (F) TIG-1 cells were infected with empty or shp53 retroviruses, and nutlin-3 was added for additional 5 days. Cells were collected 6 h after heat shock and immunoblotted for Hsp70. Interestingly, we observed an increase in basal level and after heat shock level of Hsp70 upon p53 depletion. (G) Control or p53-depleted cells were treated with 6 Gy IR and cultured for 5 days. Cells were collected 6 h after heat shock and immunoblotted for Hsp70. Abbreviations: C, age-matched healthy control; CT, control.

diated TIG-1 cells showed strong activation of p53 pathway (Fig. 1C), as well as activation of p38MAPK pathway (Fig. 2A).

To further characterize the role of the p53 signaling pathway in the suppression of HSR, we up regulated p53 without DNA damage by treating the cells with 10 μM nutlin-3, a compound that stabilizes and activates p53 (Vassilev, 2004). By day 4, early passage cells exhibited increased p53 and p21 levels, and increased SA-β-gal staining, indicating induction of the senescent phenotype (Fig. S4A,B). Induction of Hsp70 by heat shock was strongly reduced in cells treated with nutlin-3 compared to control cells (Fig. 1D), indicating that upregulation of p53 and downstream activation of the DDS even without DNA damage are sufficient for the HSR suppression.

Then we sought to determine the effects of upregulating p21, a downstream target of p53, and an important regulator of cell senescence. The p21 expression by retroviral infection in early passage cells led to the development of the senescence phenotype, which appeared 5–6 days after retroviral infection (Fig. S4A,B). As in the experiment with nutlin-3, expression of recombinant p21 caused significant decrease in induction of Hsp70 (Fig. 1E). All together, these results demonstrated that prolonged activation of the p53–p21 signaling is sufficient to suppress the HSR, (see the scheme on Fig. 6I).
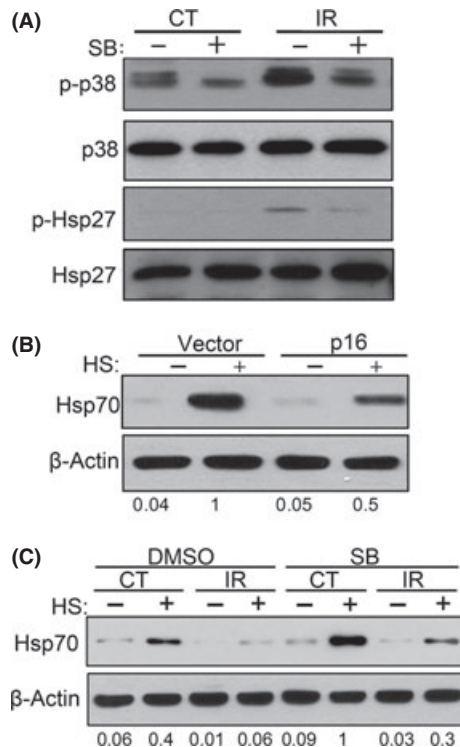
To test the possibility that inhibition of cell cycle suppresses HSR, we tested HSR in cells that have been growth arrested at G1 without activating DDS pathway, and without senescence. Accordingly, early passage TIG-1 was treated with reversible inhibitors of cyclin D/CDK4 and

Fig. 2. Activation of p38MAPK in DNA-damage-induced senescence contributes to suppression of HSR. (A) Early passage cells were pre-treated with p38MAPK inhibitor SB for 6 h prior to 10 Gy IR. After IR, cells were incubated for 6 days before collection. Levels of p–p38 and p-Hsp27 were measured by immunoblotting. (B) Hsp70 was measured after heat shock in cells with overexpression of p16. (C) Same cells as from (A) were heat shocked and incubated for 6 h before collection. Addition of SB led to partial restoration of Hsp70 induction level after heat shock.

6 complexes, 1 μM of CDK4 inhibitor (2-Bromo-12,13-dihydro-5H-indolo[2,3-a]pyrrolo[3,4-c]carbazole-5,7(6H)-dione) and 10 μM of CDK4/6 inhibitor IV (trans-4-((6-(ethylamino)-2-((1-(phenylmethyl)-1H-indol-5-yl)amino)-4-pyrimidinyl)amino)-cyclohexanol). After 3 days, treatments with either inhibitor led to G1 arrest (as judged by the G1 reporter (Sakaue-Sawano *et al.*, 2008) (Fig. S5). Similar cell cycle arrest was seen in cells overexpressing p21 or treated with nutlin-3 (Fig. S5). However, unlike the latter, cells treated with CDK inhibitors did not demonstrate SA-β-gal staining, indicating that they are not senescent (Fig. S6). Importantly, these growth-arrested but not senescent cells showed normal HSR (Fig. S7)

To examine whether the p53–p21 signaling was necessary for suppression of HSR by DDS, we depleted either of these proteins by retroviral shRNA expression. First, p53-depleted TIG-1 cells were treated with nutlin-3, as described earlier, and HSR was assessed. p53 depletion prevented p21 accumulation and the SA-β-Gal staining (Fig. S4A,C) and prevented suppression of HSR following exposure to nutlin-3 (Fig. 1F). Therefore, the inhibitory effect of nutlin-3 on HSR requires p53. More importantly, we observed reversion of HSR suppression in cells that were exposed to IR (Fig. 1G). These data demonstrated that p53 is an important factor in suppression of HSR in DNA-damage-induced senescent cells. Interestingly, p53-depleted fibroblasts showed both higher basal levels of Hsp70 and enhanced HSR compared to control empty-vector-infected cells. In contrast, depletion of p21 did not reverse the effect of nutlin-3 on HSR (Fig. S8), while, as shown earlier, expression of recombinant p21 had effectively suppressed HSR. This apparent contradiction indicated that p53 could affect HSR both via p21-dependent and p21-independent mechanisms. The p21-independent effect of p53 on HSR could result from the crosstalk between the p53 and p38MAPK pathways. In fact, we observed that nutlin-3 treatment alone caused activation of p38MAPK pathway (Fig. S9).

As such, we further investigated the contribution of the p38MAPK pathway in the suppression of HSR. In addition to the p53 pathway, IR of TIG-1 cells activated the p38MAPK signaling pathway, which plays a major role in maintenance of senescent phenotype (Rodier *et al.*, 2009). By day 5 following exposure to 10 Gy IR, we observed increased phosphorylation of p38MAPK and phosphorylation of its substrate Hsp27 (Fig. 2A). Activation of p38MAPK led to the activation of its downstream target NFκB, as measured by the NFκB luciferase reporter (Fig. S10A), which in turn caused a dramatic rise (8- to 10-fold) in mRNA levels of IL-6 and IL-8 cytokines (Fig. S10B), which are necessary for senescence maintenance. Another downstream target of the p38MAPK pathway, the cyclin-dependent kinase inhibitor p16, was also induced in TIG-1 cells following DNA damage (Fig. S11A). In line with this observation, expression of recombinant p16 led to an increased SA-β-gal staining and suppression of Hsp70 induction (Fig. 2B; Figs S3B and S11B).

To determine the role of p38MAPK in DDS-induced HSR downregulation, we tested whether this downregulation is affected by inhibition of p38MAPK activity. TIG-1 cells were exposed to 10 Gy IR and cultured for 6 days in the presence or absence of specific p38MAPK inhibitor SB203580 (SB) (Davies *et al.*, 2000). SB blocked p38MAPK kinase activity induced by IR as demonstrated by suppression of Hsp27 phosphorylation and IL-6 and IL-8 transcription (Fig. 2A; Fig. S10B). Importantly, inhibition of p38MAPK significantly improved HSR in IR-induced senescent cells (Fig. 2C). Similar to the effects on Hsp70 levels after p53 depletion, p38MAPK inhibition led to significant increase in the basal levels of Hsp70, as well. Together these data indicate that both the p53–p21 and p38MAPK–SASP pathways contribute to the downregulation of the HSR in DDS-induced senescence (see Fig. 6I).

Role of SIRT1 in regulation of Hsf1 in senescence

Next we explored which step of HSR was compromised in DDS-induced senescent cells. Activation of HSF1 and its binding to heat shock elements (HSE) is the major event to induce the transcription of Hsp70 and other heat shock proteins. To assay this activity, lentiviral reporter construct was prepared by inserting six tandem repeats of HSE upstream of firefly luciferase controlled by minimal CMV promoter. To control efficiency of infection, along with the HSE luciferase virus, we co-infected the cells with retrovirus expressing GFP under the constitutive CMV promoter. Accordingly, the ratio between HSE luciferase activity and GFP expression represented the Hsf1 activity. Luciferase activity increased by almost 30-fold in heat shocked cells (Fig. 3A). However, Dox or IR treatment prior to HS dramatically reduced (by 65–80%) the Hsf1-dependent luciferase

activity (Fig. 3A). Moreover, upregulation of one of the elements in the DDS pathways, namely p53, p21 or p16, similarly suppressed the Hsf1-driven luciferase activity (Fig. 3A). Hence, suppression of HSR in DDS-induced senescence is caused by the downregulation of Hsf1.

Here we assessed Hsf1 activity and its levels. The histone decetylase SIRT1 was previously shown to form complex with Hsf1 during heat shock and regulate its activity (Westerheide *et al.*, 2009). We hypothesized that in senescent TIG-1 fibroblasts, Hsf1 transcriptional activity was decreased because of reduced association with SIRT1.

Accordingly, we expressed FLAG-tagged Hsf1 using retroviral expression system. Hsf1 was immunoprecipitated (IP) with anti-FLAG antibody from lysates of heat-shocked control and nutlin-3-treated cells. The amount of SIRT1 in complex with Hsf1 assessed by immunoblotting with anti-SIRT1 antibody was dramatically reduced in nutlin-3-treated fibro-
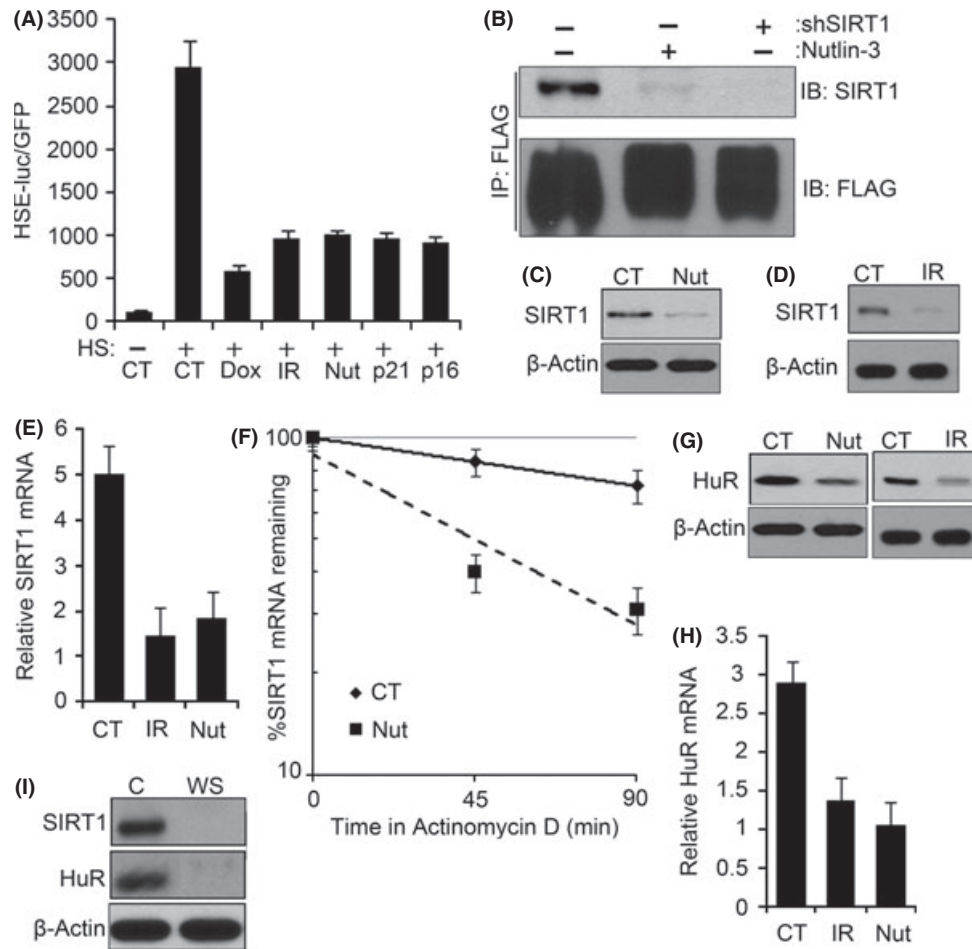
Fig. 3. DNA-damage-induced senescence suppresses Hsf1 activity by decreasing SIRT. (A) TIG-1 fibroblasts were infected with the HSE-luciferase and treated with 100 nM Dox overnight and cultured for 6 days; 10 Gy IR and cultured for 6 days; 10 μM nutlin-3 for 5 days or retroviral expression of p21 or p16 for 6 days. After heat shock, cells were incubated for 6 h before collection, and luciferase activity was measured. The means and ±SEM indicate three independent experiments. (B) FLAG-tagged wild-type Hsf1 was expressed with retrovirus in TIG-1 fibroblasts and treated with 10 μM of nutlin-3 for 5 days to induce senescence or depleted of SIRT1 by lentiviral shRNA. Cells were collected promptly after heat shock at 43 °C for 1 h, and immunoprecipitated with anti-FLAG antibody. The precipitates were immunoblotted for SIRT1. (C and D) Early passage TIG-1 fibroblasts were treated as in (A) and immunoblotted for SIRT1. (E) TIG-1 fibroblasts exposed to conditions mentioned (A) were collected for RNA, and qRT-PCR was performed using SIRT1 and GAPDH (housekeeping gene for control) mRNA-specific primers. The means and ±SEM are from three independent experiments. (F) SIRT1 mRNA half-life was measured in control (CT) and nutlin-3-induced senescent cells (Nut) by incubating with 5 μg mL^{-1} of actinomycin D and collecting RNA after 45 and 90 min. SIRT1 mRNA was normalized for GAPDH mRNA. The means and ±SEM were calculated from triplicates of two independent experiments. (G) Early passage TIG-1 fibroblasts were exposed to conditions mentioned in (A), and HuR protein levels were measured by immunoblotting. (H) HuR mRNA levels were measured by qRT-PCR, as in (F). The means and ±SEM are from three independent experiments. (I) Same set of cells as in Fig. 1(A) were immunoblotted for SIRT1 and HuR.

blasts compared to control cells (Fig. 3B). This reduction was associated with significant decrease in the SIRT1 levels (by 90%) in the nutlin-3-treated cells (Fig. 3C). Similarly, a remarkable decrease in the SIRT1 levels was observed in senescent cells induced by p21 or p16 expression and in cells subjected to IR (Fig. 3D; Fig. S12A). Thus, upon premature senescence induced by DDS, expression levels of the critical Hsf1 regulator SIRT1 are diminished.

To understand how SIRT1 is downregulated in premature senescence, we compared SIRT1 mRNA levels measured by qRT-PCR. Indeed, SIRT1 mRNA levels were reduced by 60% in the DDS-induced senescent cells compared to control (Fig. 3E; Fig. S12B), indicating that transition to senescence affects either SIRT1 transcription or stability of its mRNA. We further assessed decay of this mRNA following addition of actinomycin D to inhibit transcription. SIRT1 mRNA half-life was >5 h in control cells while in nutlin-3-induced senescent cells, half-life dropped to <45 min (Fig. 3F). This indicated that the reduction in the SIRT1 levels in prematurely senescent cells is associated with decreased mRNA stability.

Role of HuR in SIRT1-mediated regulation of Hsf1 activity in senescence

The RNA binding protein HuR (ELAV1) is the major regulator of SIRT1 mRNA stability (Abdelmohsen *et al.*, 2007). Using the shRNA approach, we confirmed that depletion of HuR in TIG-1 cells led to a dramatic drop in SIRT1 levels (Fig. S13). Because HuR levels decrease in replicative senescence (Marasa *et al.*, 2010), we hypothesized that HuR expression may also be reduced in cells that underwent senescence in response to DNA damage signaling. Indeed, HuR protein levels were significantly reduced in TIG-1 cells following treatments with Dox, IR or nutlin-3 as well as expression of p21 or p16 (Fig. 3G; Fig. S14A). In all these models of premature senescence, HuR downregulation resulted from decrease in mRNA levels (Fig. 3H; Fig. S14B). There was no significant change in half-life of HuR mRNA (Fig. S15), suggesting that effects of senescence on HuR were mostly because of transcription inhibition.

Furthermore, as shown in Fig. 3I, we observed a dramatic drop of both HuR and SIRT1 levels in WS fibroblasts suggesting that pathways of suppression of the HSR are similar in DDS-induced senescence and in the disease.

Hsf1 levels are decreased in DNA-damage signaling-induced senescence

To determine the contribution of SIRT1 in the HSR regulation in TIG-1 fibroblasts, we evaluated effects of the SIRT1 inhibitor nicotinamide on activity on Hsf1 in early passage cells. In line with previous reports, SIRT1 inhibition led to nearly 40% decrease in the Hsf1 activity measured with the HSE luciferase reporter (Fig. 4A), or by immunoblotting for Hsp70 (Fig. S16). Similarly, depletion of SIRT1 strongly (by 60%) inhibited Hsf1 activity (Fig. 4A). Analogous effect was seen in cells with depleted HuR (Fig. 4A), demonstrating that the HuR–SIRT1 pathway regulates Hsf1 in this system. Of note, treatment with nicotinamide or SIRT1 depletion did not cause premature senescence as measured by SA-β-gal or p53 and p21 (Figs S17 and S18A,B).

Beyond regulating Hsf1 activation, depletion of either HuR or SIRT1 consistently caused reduction (about 20%) of Hsf1 protein levels, suggesting that the histone deacetylase activity of SIRT1 contributes to Hsf1 expression (Fig. 4B). In line with these data, we discovered that Hsf1 expression levels were significantly decreased in TIG-1 fibroblasts treated with DNA damaging agents or nutlin-3, and in WS fibroblasts (Fig. 4B,C).

In contrast to senescent fibroblasts, lack of HSR downregulation in growth-arrested fibroblasts correlated with the lack of downregulation of HuR, SIRT1, and Hsf1 (Fig. S19). Similar correlation was seen in control and hTERT-immortalized WS fibroblasts (Fig. S20). These data further demonstrate that both Hsf1 activity and the levels are regulated in senescence in HuR–SIRT1-dependent manner. Importantly, nutlin-3 treatment had a stronger inhibitory effect on HSF1 activity (90% inhibition) and levels (40% downregulation) compared to SIRT1 or HuR depletions (Fig. 4A,B). Furthermore, combination of either of these depletions and nutlin-3 treatment did not inhibit the HSR beyond the inhibition by nutlin-3 alone (Fig. 4A,B). These results indicate that nutlin-3 treatment downregulates Hsf1 via both HuR–SIRT1-dependent and HuR–SIRT1-independent mechanisms, and the latter mechanism(s) is likely to affect Hsf1 levels.

The effects of nutlin-3 on HSR were associated with reduction of the Hsf1 mRNA (Fig. 4D), but not the stability of mRNA (Fig. 4E) or protein (not shown). Taken together, these results demonstrate that the stress-induced senescence downregulates Hsf1 via multiple mechanisms, including HuR–SIRT1 pathway, which ultimately leads to suppression of the HSR (see Fig. 6I).

Major DNA-damage signaling pathways are involved in regulation of HuR, SIRT1, and Hsf1

As DDS-induced senescence led to decreased HuR–SIRT1–Hsf1 levels, we tested whether inhibition of either p53 or p38MAPK pathways can restore levels of HuR–SIRT1 and expression of Hsf1. Depletion of p53 significantly increased the levels of HuR, SIRT1 and Hsf1 in naïve cells. Moreover, p53 depletion averted downregulation of the levels of these proteins after nutlin-3 or IR treatments (Fig. 4F; Fig. S21), indicating that p53 significantly contributed to the suppression of the HuR–SIRT1–Hsf1 pathway in senescence (see Fig. 6I). Similarly, we inhibited the p38MAPK pathway with SB and tested HuR, SIRT1 and Hsf1 levels. Cells were treated with nutlin-3 or Dox with or without SB, Dox was removed after 2 days, and all samples were grown for 5 days. Figure 4G and Figure S22(A) show that inhibition of p38MAPK increased the levels of HuR, SIRT1 and Hsf1 in naïve cells and partially restored these levels in DDS-induced senescent cells. In line with these data, we observed restoration of levels of Hsp70 (Fig. S22B,C), which further indicated that HuR–SIRT1–Hsf1 pathway can be regulated by the p38MAPK–SASP signaling (see Fig. 6I).

To investigate the relevance of these findings to the disease, we asked whether HuR–SIRT1–Hsf1 pathway can be restored in WS fibroblasts by the p38MAPK inhibition. This possibility was in line with the previously published study showing that extended inhibition of p38MAPK improved proliferation and reduced indicators of premature senescence in WS fibroblasts (Fleming *et al.*, 2005). We observed that incubation of WS fibroblasts with SB for 24 days led to a restoration of the levels of HuR, SIRT1 and Hsf1 (Fig. 4H). In these cells, we also observed an impressive restoration of HSR measured by induction of Hsp70 (Fig. 4I). These data indicate that the p38MAPK–SASP pathway contributes to suppression of Hur–SIRT1–Hsf1 pathway in WS.

HSF1 regulates HuR–SIRT1 pathway via a positive feedback

Using *C. elegans*, it was demonstrated that Hsf1 plays a major role in progression of aging: knockdown of Hsf1 accelerated this process, while overexpression delayed it (Hsu *et al.*, 2003; Ben-Zvi *et al.*, 2009; Anckar & Sistonen, 2010). The finding that SIRT1 is involved in the regulation of Hsf1 in senescence suggests that Hsf1 may act downstream and contribute to
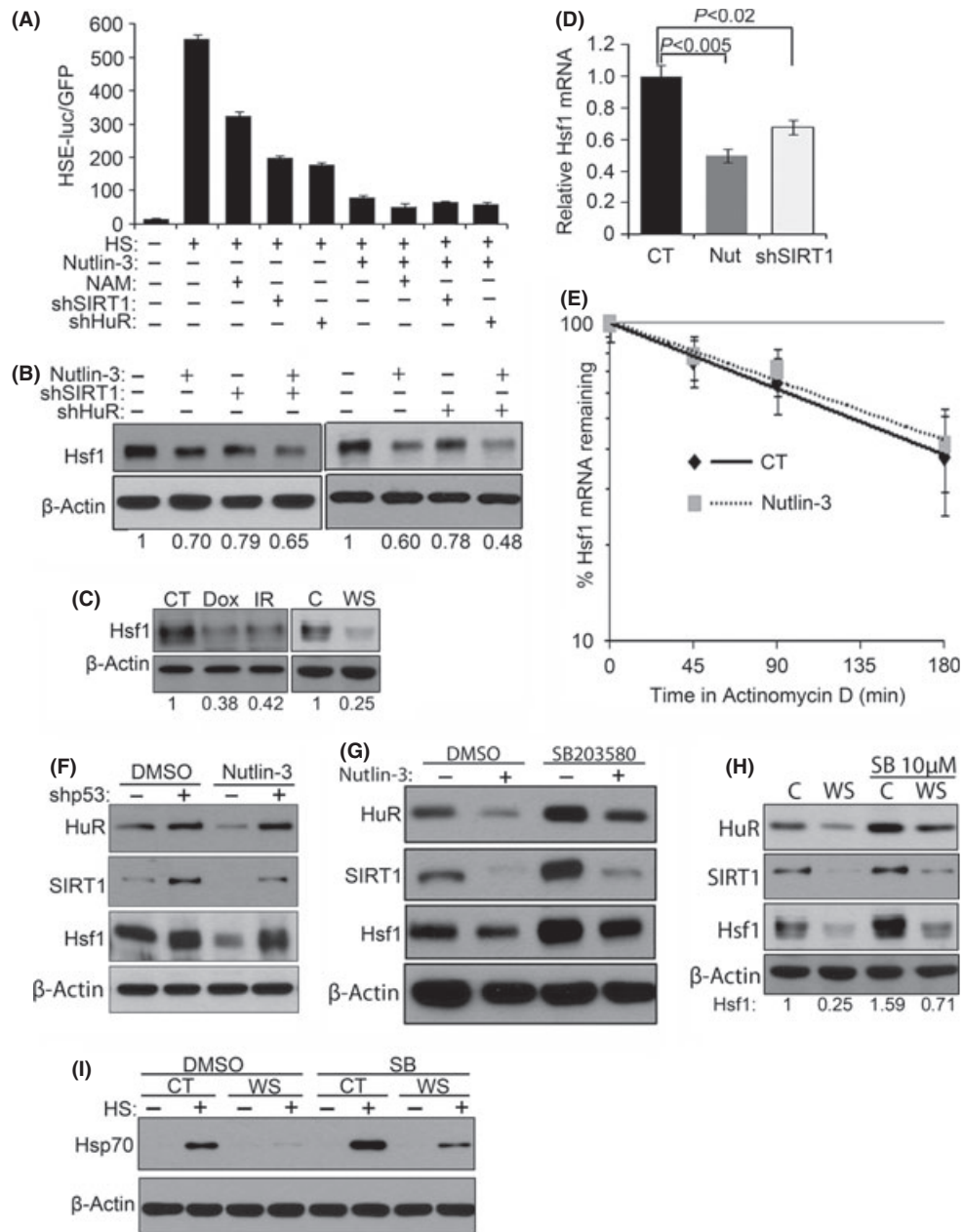
Fig. 4. Decrease in Hsf1 level in senescence is related to SIRT1 downregulation. (A) HSE-luciferase lentiviral construct was expressed in early passage cells and treated with 5 mM NAM overnight, nutlin-3 for 5 days, or infected with shRNA for SIRT1 or HuR. After heat shock, cells were incubated for 6 h before collection, and luciferase activity was measured. The means and ±SEM indicate three independent experiments. (B) Control vector or lentiviral shRNA for either SIRT1 or HuR was expressed in early passage TIG-1 fibroblasts. Cells were selected with puromycin and treated with 10 μM nutlin-3 for 5 days. Levels of Hsf1 were measured by immunoblotting. (C) Lysates of cells described in Fig. 1(A,B) were immunoblotted for Hsf1. (D) Early passage TIG-1 fibroblasts were treated with nutlin-3 to induce senescence. Cells were collected and Hsf1 mRNA levels were measured by qRT-PCR. (E) Hsf1 mRNA half-life was analyzed as in Fig. 3E. The means and ±SEM were calculated from triplicates of two independent experiments. (F) Early passage cells were infected with retroviral empty vector or shRNA against p53 and then treated with 10 μM nutlin-3 for 5 additional days. Cells lysates were immunoblotted for HuR, SIRT1, and Hsf1. (G) Early passage cells were incubated with 10 μM SB and 10 μM nutlin-3 for 5 days, and levels of HuR, SIRT1, and Hsf1 were measured. (H) 10 μM of SB was added for 24 days to WS fibroblasts, and levels of HuR, SIRT1 and Hsf1 were measured. (I) 10 μM of SB was added for 24 days to WS fibroblasts and heat shocked for 35 min at 43 °C. After 6 h incubation, cells were collected and immunoblotted for Hsp70.

anti-aging effects of SIRT1. Alternatively, there may be bi-directional relationship between SIRT1 and Hsf1. To address these possibilities, we tested the effects of Hsf1 depletion on the levels of SIRT1. Indeed, depletion of Hsf1 caused a decrease in SIRT1 protein levels by 60% and its mRNA levels by 50%, similar to the effects seen in the senescent cells (Fig. 5A,B). Furthermore, similar to its effects on SIRT1, Hsf1 depletion caused a dramatic decrease in both protein and mRNA levels of HuR (Fig. 5A,B). Thus, Hsf1 regulates the HuR–SIRT1 pathway (see Fig. 6I).

To investigate whether the discovered Hsf1 signaling occurs in vivo, we compared the levels of HuR and SIRT1 in wild-type and Hsf1 null mice. Twelve months old Hsf1 null mice and age-matched controls were sacrificed, and protein and mRNA levels of SIRT1 and HuR were
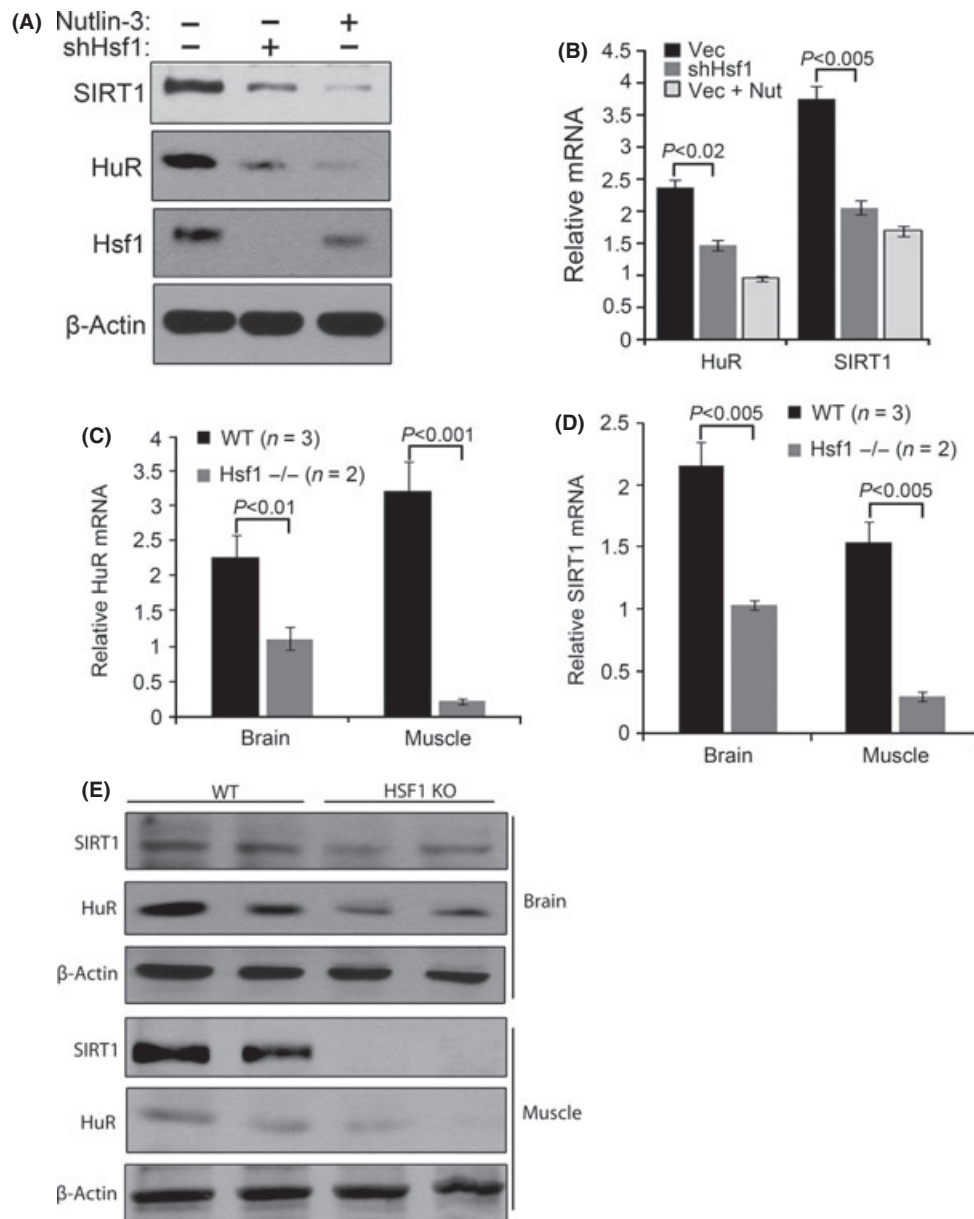
Fig. 5. Hsf1 depletion downregulates SIRT1 and HuR. (A) Retroviral control or Hsf1 shRNA were expressed in early passage TIG-1 fibroblasts. Puromycin selected cells were treated with nutlin-3 for 5 days to induce senescence. Levels of SIRT1 and HuR were measured by immunoblotting. (B) Levels of SIRT1 and HuR mRNA were measured in cells described in (A). (C and D) Brain and soleus muscles were harvested from 12 months old Hsf1 null ($-/-$) mice ($n = 2$) and age-matched control mice ($n = 3$) and preserved in RNA stable buffer. RNA from whole brain and soleus muscle were isolated, and qRT-PCR was performed with mouse HuR-, SIRT1-, and GAPDH-specific primers. (E) SIRT1 and HuR protein levels were measured by immunoblotting in samples used in C and D.

assessed in various tissues. Indeed, the levels of both SIRT1 and HuR mRNA in brain and muscle were significantly decreased in the Hsf1 null mice compared to the wild-type animals (Fig. 5C,D). Consistent with the mRNA results, Hsf1 knockout strongly decreased the levels of HuR and SIRT1 protein in the muscle and to a lesser degree in the brain (Fig. 5E). These data demonstrate that feedback regulation of SIRT1 and HuR by Hsf1 occurs at the level of organisms.

Altogether these data demonstrate that decrease in HuR–SIRT1 leads to the suppression of Hsf1, while Hsf1 suppression in turn causes downregulation of HuR and SIRT1, thus creating a positive feedback loop.

Hsf1 plays a role in regulation of DNA-damage signaling-induced senescence

How does Hsf1 signal back to regulate HuR and SIRT1 levels? Because the effects of HSF1 depletion on SIRT were similar to those seen in DDS-induced senescence, we explored effects of Hsf1 on p53 and p38MAPK signaling pathways upstream of SIRT1 and on overall senescence development. We found that depletion of Hsf1 increased a fraction of SA-β-gal-positive cells, similar to the one observed after nultin-3 treatment (Fig. 6A). Moreover, Hsf1 depletion caused senescence associated heterochromatin foci formation, further evidencing
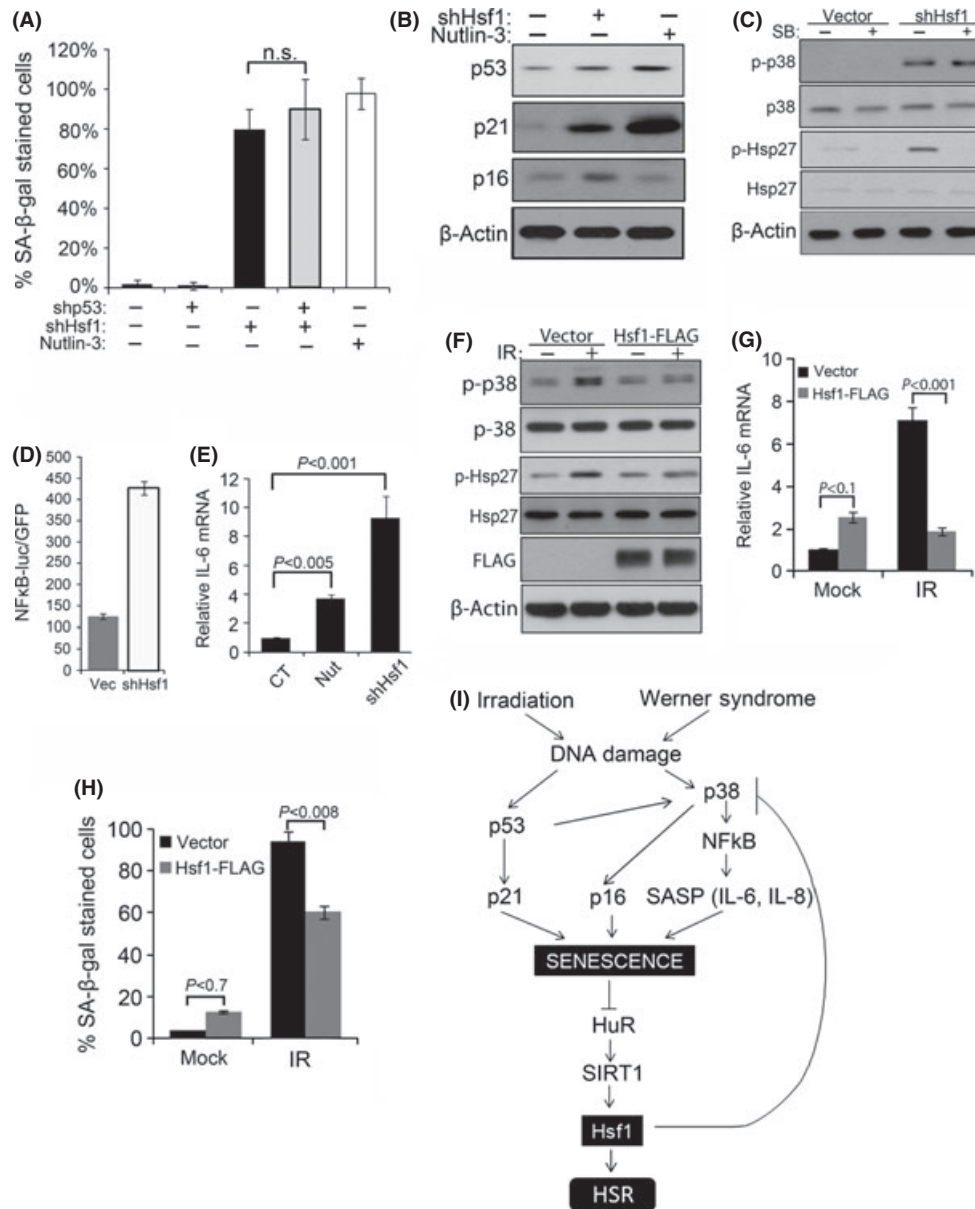
Fig. 6. Changes in Hsf1 levels modulate senescence phenotype. Retroviral control or shRNA for Hsf1 and∕or p53 were expressed in early passage TIG-1 fibroblasts and selected with puromycin. The 10 μM nutlin-3 was added for 5 days. (A) Cells were fixed and stained with SA-β-gal. The means and ±SD are from two independent experiments with 150 cell counts from four different fields. Cells were counted using images taken from bright phase microscope. (B) p53 and p21 were measured in Hsf1-depleted and nutlin-3-treated cells. (C) Control and Hsf1-depleted cells were treated with SB. The levels of p38MAPK and Hsp27 phosphorylation were measured by immunoblotting. (D) Effects of Hsf1 depletion on NF-κB. Cells were first infected with lentiviral NFκB luciferase reporter and then with retroviral empty vector or shRNA against Hsf1. First lane indicates basal luciferase activity reading without retroviral infection. (E) Control or Hsf1-depleted cells were treated with 10 μM nutlin-3, SB or vehicle for additional 5 days and IL-6 mRNA was measured. The mean and ±SEM were of three independent experiments. (F) Control of Hsf1-overexpressing cells were treated with 10 Gy IR and cultured for 6 days, and immunoblotted for indicated proteins. (G) IL-6 mRNA was measured in the same set of cells as in (F). The mean and ±SEM were from triplicates of two independent experiments. (H) Control of Hsf1-overexpressing cells was treated with 8 Gy IR and cultured for 6 days, then fixed and stained with SA-β-gal. The means and ±SD are from two independent experiments with 150 cell counts from four different fields. Cells were counted using images taken from bright phase microscope. (I) A model of relations between Hsf1 and senescence pathways. Radiation or DNA damage in WS causes activation of p53 and p38MAPK pathways. p53 induces p21 which activates senescence. Activation of p38MAPK stimulates NFκB pathway, which maintains senescence by increased production of SASP cytokines. Established senescence causes decrease in HuR, SIRT1, and Hsf1. Downregulation of Hsf1 in a feedback loop inhibits p38MAPK, which further promotes senescence and reduces levels of HuR and SIRT1.

senescence (Fig. S23). Importantly, depletion of p53 did not reverse SA-β-gal staining caused by Hsf1 depletion (Fig. 6A). Furthermore, even though we observed an upregulation of p53 and p21 in Hsf1-depleted cells, their levels were significantly lower than the levels seen in DDS-induced senescent cells (Fig. 6B). These data suggested that

the development of the senescence phenotype in Hsf1 depleted cells was independent of p53 activity and that the alternative p38MAPK–SASP pathway may be an important contributor to the feedback loop. As an indicator of p38MAPK pathway activation, levels of p16 were elevated after Hsf1 depletion (Fig. 6B).

To test whether senescence in Hsf1 depletion was mediated by increased p38MAPK activity and SASP, we explored the role of Hsf1 in regulation of this pathway. Previously, it has been demonstrated that Hsf1 can regulate IL-6 and other chemokines and that LPS-stimulated levels of IL-6 were higher in Hsf1 knockout mice than in wild-type mice (Takii et al., 2010). Here, we observed a strong increase in p38MAPK activity after Hsf1 depletion, measured by both phosphorylation of p38MAPK and phosphorylation of its substrate Hsp27 (Fig. 6C). This activation was comparable to the activation of p38MAPK by nutlin-3 (Fig. S24). Furthermore, the levels of IκB phosphorylation, which indicate activation of NFκB, as well as NFκB firefly luciferase reporter activity were increased significantly upon Hsf1 depletion (Fig. 6D; Fig. S25). As a corollary, we detected significantly increased transcription of NFκB target IL-6 (Fig. 6E). Interestingly, treatment with the p38MAPK inhibitor SB partially reversed SA-β-gal staining following Hsf1 depletion (Fig. S26). These data indicate that downregulation of Hsf1 following DNA damage signals back to the p38MAPK–SASP pathway to facilitate the maintenance of senescence (see Fig. 6I).

To further explore the role of Hsf1 in control of DDS-induced senescence pathways, we tested whether Hsf1 can suppress the activation of the p38MAPK–SASP pathway and the establishment of senescence phenotype after DNA damaging stress. Accordingly, we stably expressed FLAG-tagged Hsf1 in early passage TIG-1 cells using retroviral expression system and exposed them to IR. As a control, we used TIG-1 cells expressing an empty vector. Hsf1 strongly suppressed the IR-induced activation of p38MAPK, measured by reduced phosphorylation levels of both p38MAPK and Hsp27 (Fig. 6F). Similarly, it strongly inhibited production of IL-6 and IL-8 in the cells exposed to radiation (Fig. 6G; Fig. S27). These effects culminated in suppression of the DDS-induced senescence. In fact, we observed about 40% decrease in the fraction of SA-β-gal-positive cells in the irradiated samples (Fig. 6H). Taken together, these data demonstrate that Hsf1 plays an important role in DDS-induced senescence signaling via a positive feedback loop to regulate p38MAPK–SASP pathway (see Fig. 6I).

Discussion

This investigation provided an insight into the mechanisms of HSR suppression in DDS-induced senescence, including the multiple levels of Hsf1 regulation. Our data demonstrate that in prematurely senescent cells from patients with WS, the suppression of HSR is caused by DDS. Moreover, the activation of DDR signaling that induces senescence in early passage cells leads to significant downregulation of Hsf1 levels and activity. Here, in the first endeavor to understand the effects of senescence signaling on HSR, we demonstrated that both p53–p21 and p38MAPK–SASP pathways significantly contribute to regulation of Hsf1. Both pathways affect Hsf1 activity and levels in large part via regulation of SIRT1 levels, which in turn are controlled by the translation regulator HuR (see Fig. 6I). These effects were seen both in normal fibroblasts exposed to DNA damage and in fibroblasts from patients with WS.

A significant advance in this work is the finding that SIRT1 and Hsf1 regulate each other in a positive feedback loop. In fact, depletion of SIRT1 or HuR caused downregulation of Hsf1, while depletion of Hsf1 caused downregulation of HuR and SIRT1. As SIRT1 and Hsf1 were implicated in aging, these feedback relations may explain multiple effects of both proteins on the aging process. Importantly, the discovery of the same regulation in tissues of Hsf1 knockout mice enables us to extrapolate the implications of DNA damage at the cellular level to an organismal level.

This study also established the role of Hsf1 in regulation of the senescence-associated secretory phenotype. SASP represents a chronic inflammatory response, some components of which, for example, IL-6 or IL-1, were reported to control cell senescence. Here, we indeed demonstrate that one of the endpoints of SASP is downregulation of HuR–SIRT1, and subsequent downregulation of Hsf1. In line with these data, chronic inflammation mediated by p38MAPK was reported to play an important role in cessation of growth of WS fibroblasts, and possibly the overall acceleration of aging of patients with WS (Davis et al., 2005). Here we found that inhibition of p38MAPK partially restores Hsf1, as well as HuR and SIRT1. It is possible that such restoration may significantly improve patients' conditions.

Previously it was reported that the transcription factor C/EBPβ, which responds to SASP, can directly inhibit Hsf1 in human monocytes (Xie et al., 2002). In our system, effects of SASP are certainly distinct, because we could not detect significant effects of C/EBPβ depletion on Hsf1 activity (not shown), even though SASP was clearly associated with downregulation of HuR–SIRT1 axis.

Importantly, the feedback regulation of HuR–SIRT1 upon Hsf1 depletion is mediated by the p38MAPK–SASP pathway. This finding is consistent with previous reports that suggest enhanced inflammatory response in Hsf1 knockout animals (McMillan et al., 1998). In fact, such mice were more sensitive to LPS, and demonstrated stronger upregulation of TNF in response to LPS (Xiao et al., 1999; Takii et al., 2010). In this study, we have found the inextricable link between pro-inflammatory cytokines and Hsf1 activity. In addition to keeping the proteome in balance, Hsf1 prevents establishment of microenvironment that adversely affects the organism. This study introduces a novel perspective on the relations between proteostasis and aging. Previous reports indicated the necessity of functional Hsf1 in extension of lifespan or in decreasing onset of protein misfolding diseases, implicating the importance of proteostasis in these conditions. On the other hand, as pro-inflammatory cytokines, especially IL-6 has been linked to age-related diseases and certain types of cancer, our findings indicate that at least in part effects of Hsf1 could be associated with regulation of signaling pathways involved in chronic inflammation.

A significant finding in this work is that Hsf1 by the feedback signaling can suppress cell senescence. In fact, depletion of Hsf1 facilitated senescence, while overexpression of Hsf1 reduced DNA-damage-induced senescence. In other words, DDS via downregulation of HuR–SIRT1 pathway suppresses Hsf1, which in turn enhances the p38MAPK–SASP pathway, thus supporting chronic inflammation and senescence phenotype (Fig. 6I). These findings uncover unexpected relations between the DNA damage and proteostasis; in normal cells, the proteostasis regulator Hsf1 controls cessation of proliferation of cells with damaged DNA. It is conceivable that failure of this control in cancer cells contribute to the loss of growth cessation of cells with DNA damage/instability.

List of abbreviations: HSR - heat shock response; DDS - DNA damage-induced signaling; SASP - senescence-associated secretion phenotype; WS - Werner Syndrome; Dox - doxorubicin; IR - γ-irradiation; SA-b-gal - senescence-associated b-galactosidase activity; HSE - heat shock elements; SB - SB203580 compound.

References

Abdelmohsen K, Pullmann R, Lai A, Kim HH, Galban S, Yang XL, Blethrow JD, Walker M, Shubert J, Gillespie DA, Furneaux H, Gorospe M (2007) Phosphorylation of HuR by Chk2 regulates SIRT1 expression. *Mol. Cell* **25**, 543–557.

Acosta JC, O'Loghlen A, Banito A, Guijarro MV, Augert A, Raguz S, Fumagalli M, Da Costa M, Brown C, Popov N, Takatsu Y, Melamed J, di Fagagna FD, Bernard D, Hernando E, Gil J (2008) Chemokine signaling via the CXCR2 receptor reinforces senescence. *Cell* **133**, 1006–1018.

Anckar J, Sistonen L (2010) Regulation of HSF1 function in the heat stress response: implications in aging and disease. *Annu. Rev. Biochem.* **80**, 1089–1115.

Ben-Zvi A, Miller EA, Morimoto RI (2009) Collapse of proteostasis represents an early molecular event in *Caenorhabditis elegans* aging. *Proc. Nat. Acad. Sci. U.S.A.* **106**, 14914–14919.

Chang BD, Xuan YZ, Broude EV, Zhu HM, Schott B, Fang J, Roninson IB (1999) Role of p53 and p21(waf1∕cip1) in senescence-like terminal proliferation arrest induced in human tumor cells by chemotherapeutic drugs. *Oncogene* **18**, 4808–4818.

Davies SP, Reddy H, Caivano M, Cohen P (2000) Specificity and mechanism of action of some commonly used protein kinase inhibitors. *Biochem. J.* **351**, 95–105.

Davis T, Baird DM, Haughton MF, Jones CJ, Kipling D (2005) Prevention of accelerated cell aging in Werner syndrome using a p38 mitogen-activated protein kinase inhibitor. *J. Gerontol. A Biol. Sci. Med. Sci.* **60**, 1386–1393.

Du ZX, Zhang HY, Meng X, Gao YY, Zou RL, Liu BQ, Guan Y, Wang HQ (2009) Proteasome inhibitor MG132 induces BAG3 expression through activation of heat shock factor 1. *J. Cell. Physiol.* **218**, 631–637.

Fan XHC, Steitz JA (1998) Overexpression of HuR, a nuclear-cytoplasmic shuttling protein, increases the in vivo stability of ARE-containing mRNAs. *EMBO J.* **17**, 3448–3460.

Fleming JB, Shen G-L, Holloway SE, Davis M, Brekken RA (2005) Molecular consequences of silencing mutant K-ras in pancreatic cancer cells: justification for K-ras-directed therapy. *Mol. Cancer Res.* **3**, 413–423.

Freund A, Patil CK, Campisi J (2011) p38MAPK is a novel DNA damage response-independent regulator of the senescence-associated secretory phenotype. *EMBO J.* **30**, 1536–1548.

Goto M (1997) Hierarchical deterioration of body systems in Werner's syndrome: Implications for normal ageing. *Mech. Ageing Dev.* **98**, 239–254.

Heydari AR, Wu B, Takahashi R, Strong R, Richardson A (1993) Expression of heat shock protein 70 is altered by age and diet at the level of transcription. *Mol. Cell. Biol.* **15**, 2909–2918.

Heydari AR, Takahashi R, Gutsmann A, You S, Richardson A (1994) Hsp70 and aging. *Experientia* **50**, 1092–1098.

Hsu AL, Murphy CT, Kenyon C (2003) Regulation of aging and age-related disease by DAF-16 and heat-shock factor. *Science* **300**, 1142–1145.

Jana NR, Tanaka M, Wang GH, Nukina N (2000) Polyglutamine length–dependent interaction of Hsp40 and Hsp70 family chaperones with truncated N-terminal huntingtin: their role in suppression of aggregation and cellular toxicity. *Hum. Mol. Genet.* **9**, 2009–2018.

Koyama S, Arawaka S, Chang-Hong R, Wada M, Kawanami T, Kurita K, Kato M, Nagai M, Aoki M, Itoyama Y, Sobue G, Chan PH, Kato T (2006) Alteration of familial ALS-linked mutant SOD1 solubility with disease progression: Its modulation by the proteasome and Hsp70. *Biochem. Biophys. Res. Commun.* **343**, 719–730.

Lee YK, Manalo D, Liu AYC (1996) Heat shock response, heat shock transcription factor and cell aging. *Biol. Signals* **5**, 180–191.

Marasa BS, Srikantan S, Martindale JL, Kim MM, Lee EK, Gorospe M, Abdelmohsen K (2010) MicroRNA profiling in human diploid fibroblasts uncovers miR-519 role in replicative senescence. *Aging (Albany NY)* **2**, 333–343.

McMillan DR, Xiao X, Shao L, Graves K, Benjamin IJ (1998) Targeted disruption of heat shock transcription factor 1 abolishes thermotolerance and protection against heat-inducible apoptosis. *J. Biol. Chem.* **273**, 7523–7528.

Morley JF, Morimoto RI (2004) Regulation of longevity in *Caenorhabditis elegans* by heat shock factor and molecular chaperones. *Mol. Biol. Cell* **15**, 657–664.

Orjalo AV, Bhaumik D, Gengler BK, Scott GK, Campisi J (2009) Cell surface-bound IL-1 alpha is an upstream regulator of the senescence-associated IL-6/IL-8 cytokine network. *Proc. Nat. Acad. Sci. U.S.A.* **106**, 17031–17036.

Rahman MM, Stuchlick O, El-Karim EG, Stuart R, Kipreos ET, Wells L (2010) Intracellular protein glycosylation modulates insulin mediated lifespan in *C. elegans*. *Aging (Albany NY)* **2**, 678–690.

Robles SJ, Adami GR (1998) Agents that cause DNA double strand breaks lead to p16(INK4a) enrichment and the premature senescence of normal fibroblasts. *Oncogene* **16**, 1113–1123.

Rodier F, Coppe JP, Patil CK, Hoeijmakers WAM, Munoz DP, Raza SR, Freund A, Campeau E, Davalos AR, Campisi J (2009) Persistent DNA damage signalling triggers senescence-associated inflammatory cytokine secretion. *Nat. Cell Biol.* **11**, U973–U142.

Rossi ML, Ghosh AK, Bohr VA (2010) Roles of Werner syndrome protein in protection of genome integrity. *DNA Repair (Amst.)* **9**, 331–344.

Sakaue-Sawano A, Kurokawa H, Morimura T, Hanyu A, Hama H, Osawa H, Kashiwagi S, Fukami K, Miyata T, Miyoshi H, Imamura T, Ogawa M, Masai H, Miyawaki A (2008) Visualizing spatiotemporal dynamics of multicellular cell-cycle progression. *Cell* **132**, 487–498.

Sakellariou GK, Pye D, Vasilaki A, Zibrik L, Palomero J, Kabayo T, McArdle F, Van Remmen H, Richardson A, Tidball JG, McArdle A, Jackson MJ (2011) Role of superoxide–nitric oxide interactions in the accelerated age-related loss of muscle mass in mice lacking Cu, Zn superoxide dismutase. *Aging Cell* **10**, 749–760.

Sasaki T, Maier B, Bartke A, Scrable H (2006) Progressive loss of SIRT1 with cell cycle withdrawal. *Aging Cell* **5**, 413–422.

Sherman MY, Goldberg AL (2001) Cellular defenses against unfolded proteins: a cell biologist thinks about neurodegenerative diseases. *Neuron* **29**, 15–32.

Takii R, Inouye S, Fujimoto M, Nakamura T, Shinkawa T, Prakasam R, Tan K, Hayashida N, Ichikawa H, Hai T, Nakai A (2010) Heat shock transcription factor 1 inhibits expression of IL-6 through activating transcription factor 3. *J. Immunol.* **184**, 1041–1048.

Taylor RC, Dillin A (2011) Aging as an event of proteostasis collapse. *Cold Spring Harb. Perspect. Biol.* **3**, pii:a004440.

Vassilev LT (2004) Small-molecule antagonists of p53-MDM2 binding: research tools and potential therapeutics. *Cell Cycle* **3**, 419–421.

Vaziri H, West MD, Allsopp RC, Davison TS, Wu YS, Arrowsmith CH, Poirier GG, Benchimol S (1997) ATM-dependent telomere loss in aging human diploid fibroblasts and DNA damage lead to the post-translational activation of p53 protein involving poly(ADP-ribose) polymerase. *EMBO J.* **16**, 6018–6033.

Westerheide SD, Anckar J, Stevens SM Jr, Sistonen L, Morimoto RI (2009) Stress-inducible regulation of heat shock factor 1 by the deacetylase SIRT1. *Science* **323**, 1063–1066.

Wu B, Gu MJ, Heydari AR, Richardson A (1993) The effect of age on the synthesis of 2 heat-shock proteins in the Hsp70 family. *J. Gerontol.* **48**, B50–B56.

Wyllie FS, Jones CJ, Skinner JW, Haughton MF, Wallis C, Wynford-Thomas D, Faragher RGA, Kipling D (2000) Telomerase prevents the accelerated cell ageing of Werner syndrome fibroblasts. *Nat. Genet.* **24**, 16–17.

Xiao X, Zuo X, Davis AA, McMillan DR, Curry BB, Richardson JA, Benjamin IJ (1999) HSF1 is required for extra-embryonic development, postnatal growth and protection during inflammatory responses in mice. *EMBO J.* **18**, 5943–5952.

Xie Y, Chen CM, Stevenson MA, Hume DA, Auron PE, Calderwood SK (2002) NF-IL6 and HSF1 have mutually antagonistic effects on transcription in x3monocytic cells. *Biochem. Biophys. Res. Commun.* **291**, 1071–1080.

Supporting information

Additional supporting information may be found in the online version of this article:

Data S1 Materials and methods.

Fig. S1 Werner Syndrome fibroblasts (passage 4) exhibited prematurely senescent phenotype when compared to age matched controls (passage 15).

Fig. S2 HSR was compared in two lines of hTERT-immortalized control (CT1 and CT2) and WS (WS1 and WS2) fibroblasts. Cells were exposed to heat shock and immunoblotted for Hsp70. The normalized density of the Hsp70 band is shown below.

Fig. S3 (A) Early passage TIG-1 fibroblasts were treated with 10 Gy IR and cultured for 6 days. Cells were fixed, stained with rabbit anti-Ki-67 antibody and anti-rabbit IgG conjugated with Texas-Red secondary antibody. Images were acquired with Axiovert 200 (Carl Zeiss, Oberkochen, Germany) microscope with an ×100 objective using the manufacturer's software. Radiation decreased % of cells with Ki-67 staining. (B) Early passage cells were treated with 100 nM Dox or 10 Gy IR and cultured for 5 additional days. DNA damage caused increased SA-β-gal staining.

Fig. S4 Cells were infected with empty vector, retroviral shRNA for p53 or recombinant p21. Two days post infection, 10 μM nutlin-3 was added for additional 5 days. (A) nutlin-3 treatment or expression of p21 caused increased staining with SA-β-gal, whereas p53 depletion prevented staining

in nutlin-3 treated cells. (B) Nutlin-3 treatment led to accumulation p53 and p21 without directly causing DNA damage, and did not cause p16 upregulation. (C) Depletion of p53 prevented p21 accumulation after nutlin-3 or 6 Gy IR treatment.

Fig. S5 Early passage TIG-1 was infected with empty vector or p21 retrovirus. Next day, vector expressing cells were treated with 10 μM of nutlin-3 for 3 days or left untreated. Then all cells were infected with lentiviral cell cycle reporters, green fluorescent tagged mutant Cdt for G1 and red fluorescent tagged mutant Geminin for G2. Next day, untreated vector cells were exposed to 1 μM CDK4 inhibitor or 10 μM CDK4/6 inhibitor IV. After 3 days, cells were fixed. Fluorescent cells under RFP indicate G2 and FITC indicate G1.

Fig. S6 Cells treated with 1 μM CDK4 inhibitor or 10 μM CDK4/6 inhibitor IV for 3 days were fixed and stained with SA-β-gal.

Fig. S7 Same cells from S6 and nutlin-3 treated cells were collected 6 h after heat shock and immunoblotted for Hsp70.

Fig. S8 Early passage TIG-1 was infected with empty vector or shRNA against p21 and 2 days later treated with 10 μM nutlin-3. p21 depletion did not restore the level of Hsp70 accumulation after nutlin-3.

Fig. S9 Cells treated with nutlin-3 was incubated with or without 10 μM SB for 5 days. Cell lysates were immunoblotted for phosphorylated forms of p38MAPK and Hsp27.

Fig. S10 (A) Cells with lentiviral NFκB luciferase reporter was treated with 10 Gy IR and 3 days later infected with either lentiviral empty vector or shRelA and selected. 6 days after IR, cells were collected for luciferase assay. The means and ±SEM indicate three independent experiments. (B) Cells treated as (A) were collected for RNA. qRT-PCR was performed using IL-6, IL-8 and GAPDH mRNA. IL-6 and IL-8 mRNA dramatically increased in IR treated cells and SB inhibited the induction. The mean and ±SEM were from triplicates of two independent experiments.

Fig. S11 (A) Cells treated with 10 Gy IR was lysed and immunoblotted for p16. IR increased p16 levels. (B) Same cells as (A) were fixed and stained for SA-βgal.

Fig. S12 (A) Cells were treated with 100 nM Dox overnight and cultured for 6 days or retroviral expression of p21 or p16 for 6 days, and immunoblotted for SIRT1. SIRT1 decreased after DNA damage induced senescence. (B) Same set of cells as (A) were collected for RNA and qRT-PCR was performed using SIRT1 and GAPDH (housekeeping gene for control) mRNA specific primers. As in protein, SIRT1 mRNA was significantly decreased in senescent cells. The means and ±SEM are from three independent experiments. Abbreviations: CT, control; Vec, vector.

Fig. S13 Early passage TIG-1 was infected with lentiviral empty vector or shRNAs against HuR and SIRT1. Two days post infection, 10 μM nutlin-3 was added for additional 5 days. Nutlin-3 treatment alone decreased SIRT1 and HuR. HuR depletion caused SIRT1 decrease, whereas SIRT1 depletion did not cause HuR decrease (not shown).

Fig. S14 (A) Cells were treated with 100 nM Dox overnight and cultured for 6 days or retroviral expression of p21 or p16 for 6 days, and immunoblotted for HuR. HuR decreased after DNA damage induced senescence. (B) Same set of cells as (A) were collected for RNA and qRT-PCR was performed using HuR and GAPDH (housekeeping gene for control) mRNA specific primers. As in protein, HuR mRNA was significantly decreased in senescent cells. The means and ±SEM are from three independent experiments. Abbreviations: CT, control; Vec, vector.

Fig. S15 HuR mRNA half-life was measured in control and nutlin-3 induced senescent cells by incubating with 5 μg mL^{-1} of actinomycin D and collecting RNA after 45 and 90 min. HuR and GAPDH mRNA were measured qRT-PCR and normalized by GAPDH mRNA. Data is represented by percentage of HuR mRNA measured at time 0 min (prior to adding actinomycin D), in semi-logarithmic scale. Half-life is calculated as time need for 50% reduction of mRNA. The means and ±SEM was calculated from triplicates of two independent experiments.

Fig. S16 Early passage TIG-1 was treated with 10 μM nutlin-3 for 5 days and 5 mM nicotinamide was added overnight before heat shock. Cell lysates were immunoblotted for Hsp70. Nicotinamide suppressed Hsp70 induction in early TIG-1 fibroblasts as nutlin-3 treatment.

Fig. S17 Cells from S16 were immunoblotted for HuR, SIRT1, p53 and p21. Overnight nicotinamide treatment did not cause decrease HuR and SIRT1, and did not induce senescence by p53–p21.

Fig. S18 (A) Early passage TIG-1 was infected with lentiviral shRNA against SIRT1 and 2 days later incubated with 10 μM nutlin-3 for 5 additional days. SIRT1 depletion alone did not cause increase in p53 and p21. (B) Same set of cells as (A) were fixed and stained with SA-β-gal. SIRT1 depletion alone did not cause increased staining of SA-β-gal.

Fig. S19 Same set of cells as S7 were probed for SIRT1, HuR and Hsf1.

Fig. S20 Same set of cells as S2 were probed for SIRT1, HuR and Hsf1.

Fig. S21 TIG-1 cells were infected with retroviral empty vector or shRNA against p53 and treated with 6 Gy IR. After 5 days post IR, cells were lysed and immunoblotted for HuR, SIRT1 and Hsf1. p53 depletion increased basal level of HuR, SIRT1 and Hsf1, and prevented senescence associated decrease of those proteins.

Fig. S22 (A) Early passage cells were pre-incubated with 10 μM SB for 6 h then co-incubated with 100 nM Dox for 2 days. After removing Dox, SB was added for the additional 4 days. Administration of SB to Dox treated cells led to partial restoration of HuR, SIRT1 and Hsf1. (B) Same set of cells as (A) were heat shocked and incubated for 6 h before collection for immunoblotting for Hsp70. Administration of SB to Dox treated cells led to partial restoration of Hsp70 induction. (C) Early passage cells were incubated with 10 μM SB and 10 μM nutlin-3 for 5 days. Cells were heat shocked the incubated for 6 h before collection for immunoblotting for hsp70. Concomitant administration of SB and nutlin-3 led to partial restoration of Hsp70 induction. Abbreviations: CT, control; Nut, Nutlin-3.

Fig. S23 Early passage TIG-1 was infected with retroviral empty vector or shRNA against Hsf1. Two days later vector cells were treated with 10 μM nutlin-3 or 100 nM Dox, and cultured for 5 additional days. Cells were fixed and stained with DAPI. Arrows indicate cells with punctate DNA foci containing cells, which are senescence associated heterochromatin foci (SAHF).

Fig. S24 Early passage TIG-1 was infected with retroviral empty vector or shRNA against Hsf1, and 2 days later 10 μM nutlin-3 was added to the vector for 5 additional days. Hsf1 depletion increased phosphorylation of Hsp27, similar to nutlin-3 treated cells. Abbreviations: CT, control; Nut, Nutlin-3.

Fig. S25 Early passage TIG-1 was infected with retroviral empty vector or shRNA against Hsf1, and 2 days later 10 μM SB was added 3 additional days, and collected for immunoblotting. Hsf1 depletion increased phosphorylation of IκB. SB treatment decreased phosporylation of IκB in both vector and Hsf1 depleted cells.

Fig. S26 Early passage TIG-1 was infected with retroviral empty vector or shRNA against Hsf1, and 2 days later 10 μM SB was added for 3 additional days. Hsf1 depletion increased SA-β-gal staining, which was decreased by SB treatment.

Fig. S27 Cell expressing empty or FLAG-tagged wild-type Hsf1 were treated with 10 Gy of IR and cultured for 6 days. Cells were collected for RNA. qRT-PCR was performed using IL-8 and GAPDH mRNA. IL-8 mRNA dramatically increased in DNA damage induced senescent cells. This increase was significantly suppressed in Hsf1 expressed cells. The mean and ±SEM were from triplicates of two independent experiments.

As a service to our authors and readers, this journal provides supporting information supplied by the authors. Such materials are peer-reviewed and may be re-organized for online delivery, but are not copy-edited or typeset. Technical support issues arising from supporting information (other than missing files) should be addressed to the authors.